Numerical Computation of Compressible Fluid Flows

Amit Shivaji Dighe

A Dissertation Submitted to
Indian Institute of Technology Hyderabad
In Partial Fulfillment of the Requirements for
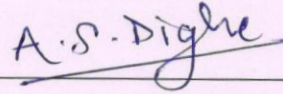The Degree of Master of Technology

भारतीय प्रौद्योगिकी संस्थान हैदराबाद
Indian Institute of Technology Hyderabad

Department of Mechanical Engineering

July, 2012

Declaration

I declare that this written submission represents my ideas in my own words, and where others' ideas or words have been included, I have adequately cited and referenced the original sources. I also declare that I have adhered to all principles of academic honesty and integrity and have not misrepresented or fabricated or falsified any idea/data/fact/source in my submission. I understand that any violation of the above will be a cause for disciplinary action by the Institute and can also evoke penal action from the sources that have thus not been properly cited, or from whom proper permission has not been taken when needed.
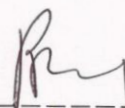
A.S. Dighe

(Signature)
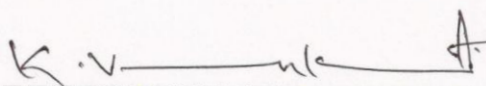
(Amit Shivaji Dighe)

(ME10M02)

Approval Sheet

This thesis entitled 'Numerical Computation of Compressible Fluid Flows' by Amit Shivaji Dighe is approved for the degree of Master of Technology from IIT Hyderabad.
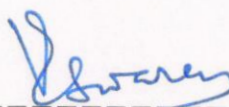
(Dr. Raja Banerjee) Examiner

Dept. of Mechanical Engg.

IITH

(Dr. K. Venkatasubbaiah) Examiner

Dept. of Mechanical Engg.

IITH

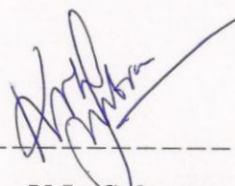(Prof. Vinayak Eswaran) Adviser

Dept. of Mechanical Engg.

IITH

(Prof. Kolluru V.L. Subramaniam) Chairman

Dept. of Civil Engg.

IITH

Acknowledgements

Dedicated to

My beloved family

Abstract

The physical behavior of compressible fluid flow is quite different from incompressible fluid flow. Compressible fluid flows encounter discontinuities such as shocks; and their solution is complicated by the hyperbolic nature of the governing equations.

In the present study the MacCormack scheme with Jameson's and TVD artificial viscosity has been implemented to solve the 2D Euler equation. One dimensional problems such as flows in a shock tube, Quasi 1D nozzle problems with transition from subsonic to supersonic, subsonic to subsonic flow, with and without shocks, have also been solved in the preliminary portion of the study. Test cases of external flow over a NACA 0012 airfoil for different inlet Mach numbers have been attempted and validated. An unsuccessful attempt was being made to implement variants of MacCormack scheme in explicit and semi implicit form.

Nomenclature

ρ	Density
u	Component of velocity in x-direction
v	Component of velocity in y-direction
a	Speed of sound
t	time
p	Pressure
T	Temperature
e	Internal energy per unit volume
E	Total energy per unit mass
w	conservative variable
f	Component of flux in x-direction
g	Component of flux in y-direction
F_f	Flux

Contents

Chapter 1

Introduction

Compressible fluid flow is a variable density fluid flow; while this variation in density could be due to both in pressure and temperature. Compressible flows (in contrast to variable density flows) are those where dynamics (i.e pressure) is a greater factor in density change. Generally fluid flow is considered to be compressible if the change in density relative to the stagnation density is greater than 5 %. Compressible effects are occurs at Mach number of 0.3. Compressible effects are observed in practical applications like high speed aerodynamics, missile and rocket propulsion, high speed turbo compressors, steam and gas turbines.

Compressible flow is divided often into four main flow regimes based on the local Mach number (M) of the fluid flow

(1) Subsonic flow regime (M <= 0.8)

(2) Transonic flow regime (0.8 <= M <= 1.2)

(3) Supersonic flow regime (M > 1)

(4) Hypersonic flow regime (M > 5)

Compressible flow may be treated as either viscous or inviscid. Viscous flows are solved by the Navier stokes system of equations and inviscid compressible flows are solved by Euler equations. Physical behavior of compressible fluid flow is quite different from the incompressible fluid flow. Compressible flow can encounter discontinuities such as shock waves. The solutions of Euler equation are different due to hyperbolic nature, from the solutions of the Elliptic governing equations of incompressible flows. So for compressible flows containing discontinuities special attention is required for solution methods which will accurately capture these discontinuities.

A major difference between solution methods for compressible flow and incompressible flow lies in the way the boundary conditions are imposed. In compressible flow boundary conditions are imposed based on the characteristic waves coming into or going out of the domain boundary, which is very different from the Elliptic-type boundary conditions used in for incompressible flows.

1.1   Literature review

Compressible fluid flow has been an area of research from many decades. Fundamental concepts of compressible fluid flow are discussed by authors such as Culbert Laney [1], J .D. Anderson [2], Charles Hirsch [3] , and T . J. Chung [4],who describe different numerical techniques and, most importantly for compressible fluid flow discuss the boundary conditions that should be used at various boundaries . These books compile the work of the many people who worked to develop different schemes for accurately simulating the compressible fluid flow. Lax-Friendrichs (1954) developed the Lax-Friendrichs scheme [5-7] and MacCormack (1969) developed the MacCormack scheme [8-10]. Flux vector splitting schemes were developed by many scientists like Courant, Isaacson, and Reeves [11], Steger and Warming [12], Van Leer [13].Godunov and Roe worked on Riemann solvers.

Euler equations suffer from numerical instability, due to lack of the stabilizing viscous terms. This was addressed in early work by adding viscosity artificially to the discretized equations. So the MacCormack scheme with Jameson artificial viscosity was used by many researchers to solve practical problems. Another modification to original MacCormack scheme is the modified Causon's scheme [18], which is based on the classical MacCormack FVM scheme in total variation diminishing (TVD) form.

Pavel and Karel [14] studied numerical solutions of system of Euler equations describing steady two dimensional inviscid compressible flow flows in 2D channels using the MacCormack scheme with Jameson artificial viscosity. The cases they studied include flow in a GAMM channel and flow around half DCA 18% profile. They concluded that the results obtained by this method are in good agreement with the other authors' results.

Petra Puncochárová-Porízková et. al [15] used MacCormack with Jameson artificial viscosity to simulate 2D unsteady flow of a compressible viscous fluid flow in the human vocal tract.

Faurst et.al [16] used a TVD-MacCormack scheme for solving flows through channel and transonic flow through the 2D turbine cascade. Jan Vimmr [17] studied mathematical modeling of complex clearance flow in 2D models of a male rotor-housing gap and of an undesirable gap caused by incorrect contact of rotor teeth in a screw type machine using the TVD-MacCormack scheme. This study was without shock waves typically for flows at macro channels.

1.2   Objective of the present work

1. To develop a two dimensional solver using the explicit MacCormack scheme with Jameson artificial viscosity to solve compressible fluid flow problems. The fluid flow problems should subsonic to subsonic flow, subsonic to supersonic flow ,supersonic to subsonic flow and supersonic to supersonic flows, and containing shocks and discontinuities.

2. Study different schemes such as TVD-MacCormack, explicit Variant MacCormack scheme and semi implicit Variant MacCormack scheme.

3. To validate the code by comparing results with those obtained using the analytical solutions and solution given in the literature.

1.3   Thesis organization

Thesis is organized in the following way. Chapter 2 deals with the governing equations and numerical schemes with discretization procedure. Chapter 3 includes boundary conditions for compressible fluid flow. Chapter 4 deals with results and discussion.

Chapter 2

Governing Equations and Numerical Schemes

2.1   Governing Equations

Euler equations describe the most general flow configuration for a non-viscous, non-heat conducting compressible fluid. These equations can be obtained from the Navier-Stokes equations by neglecting all shear stresses and heat conduction terms. However, there is drastic change in mathematical nature of the Euler equation when compared to Navier-Stokes equation. This is because the system of partial differential equation describing the inviscid flows not only, but in doing so becomes hyperbolic in contrast to the original Parabolic-Elliptic form. Therefore the boundary conditions to be imposed will be dependent upon the characteristic variable entering and leaving the domain, quite different from the Navier-Stokes equation. The Euler equations in conservative form and in absolute frame of reference are as follows

$$\frac{\partial w}{\partial t} + \vec{\nabla} \bullet \vec{F} = Q \tag{2.1}$$

This is system of first order hyperbolic partial differential equations, where the flux vector F has the Cartesian components (f, g) given by

$$w = \begin{Bmatrix} \rho \\ \rho u \\ \rho v \\ \rho E \end{Bmatrix} \qquad f = \begin{Bmatrix} \rho u \\ \rho u^2 + p \\ \rho uv \\ \rho uH \end{Bmatrix} \qquad g = \begin{Bmatrix} \rho v \\ \rho uv \\ \rho v^2 + p \\ \rho vH \end{Bmatrix} \tag{2.2}$$

Here ρ is the density, u and v are the velocities in x and y directions. p is the pressure. E is the total energy per unit mass and H is the total enthalpy per unit mass.

$$E = e + \left(\frac{u^2 + v^2}{2} \right) \qquad\qquad H = E + \frac{p}{\rho} \qquad (2.3)$$

where e is internal energy per unit volume. In the absence of heat sources, the entropy equation for continuous flow is as follows

$$T \left(\frac{\partial s}{\partial t} + \vec{u} \bullet \vec{\nabla} s \right) = 0 \qquad (2.4)$$

which implies that entropy is constant along a flow path. Hence, the Euler equations describe isentropic flows. The set of Euler equations also allows discontinuous solutions in certain cases, namely, vortex sheets, contact discontinuities or shock waves occurring in supersonic flows. These discontinuous solutions can only be obtained from the integral form of the conservation equations, since the gradients of the fluxes are not defined at discontinuity surfaces.

In order to close this system of equations for perfect gas flow, the equation of state is the perfect gas law :

$$p = \rho R T \qquad (2.5)$$

These set of equations can now be solved simultaneously in order to get density, velocity and total energy in the flow field.

2.2   Numerical Schemes

Real flow includes rotational, non-isentropic, and non-isothermal effects. Compressible inviscid flow including such effects requires simultaneous solution of continuity, momentum, and energy equations. Special computational schemes are required to resolve the shock discontinuities encountered in transonic flow. The most basic requirement for the solution of the Euler equations is to ensure that solution schemes provide an adequate amount of artificial viscosity required for rapid convergence towards a solution.

Numerical schemes to solve Euler equations may be grouped into three major categories: (1) central schemes, (2) first order upwind schemes, and (3) second order upwind schemes and essentially non-oscillatory (ENO) schemes.

2.2.1 Central schemes

These schemes are combined space-time integration schemes.

    a) Explicit schemes

        1. Lax- Friendrichs- First order scheme

        2. Lax- Wendroff –Second order scheme.

    b) Two-step Explicit schemes

        1. Richtmyer and Morton scheme

        2. MacCormack scheme

2.2.2 First order upwind schemes

    a) Multiple Flux vector splitting method.

        1. Steger and Warming method

        2. Van Leer method.

    b) Godunov methods.

2.2.3 Second order upwind schemes

        1. Variable extrapolation

        2. TVD (Total variation diminishing) scheme

In the present study the MacCormack scheme has been chosen to solve Euler equations, since it is very robust and tested scheme.

2.3 MacCormack Scheme

MacCormack scheme is a Predictor –Corrector variant of a Lax-Wendroff scheme and is much simple in its application. MacCormack is among the easiest to understand and program. MacCormack scheme is second order accurate in both space and time. Moreover, the results obtained by using MacCormack scheme are perfectly satisfactory for many fluid flow applications. For these reasons, this scheme is used in the present study.

Consider one dimensional Euler equation

$$\frac{\partial w}{\partial t} + \frac{\partial F}{\partial x} = 0 \qquad (2.6)$$

Method 1:-

Predictor step:-

$$w_i^* = w_i^n - \frac{\Delta t}{\Delta x}\left(F_{i+1}^n - F_i^n\right)$$
(2.7)

Corrector step:-

$$w_i^{n+1} = \frac{1}{2}\left(w_i^n + w_i^* - \frac{\Delta t}{\Delta x}\left(F_i^* - F_{i-1}^*\right)\right)$$
(2.8)

In this form, the predictor equation is FTFS (forward-time, forward-space). The corrector equation is FTBS (forward-time, backward-space). The predictor and corrector in MacCormack method can be reversed as follows.

Method 2:

Predictor step:-

$$w_i^* = w_i^n - \frac{\Delta t}{\Delta x}\left(F_i^n - F_{i-1}^n\right)$$
(2.9)

Corrector step:-

$$w_i^{n+1} = \frac{1}{2}\left(w_i^n + w_i^* - \frac{\Delta t}{\Delta x}\left(F_{i+1}^* - F_i^*\right)\right)$$
(2.10)

This too is again called MacCormack scheme. Left-running waves are better captured by the first version of MacCormack scheme, whereas right-running waves are better captured by the second version. In the case of MacCormack scheme, the predictor or corrector or both are always unconditionally unstable, and yet the sequence is completely stable provided only that the CFL condition is satisfied i.e. *Courant no ≤ 1.*

2.4   MacCormack Scheme

After non-dimensionalising the Euler equations by following non-dimensionalising parameters equations (2.1-2.2) in 2 dimensional form is as follows

$$T^{'} = \frac{T}{T_0} \ , \quad \rho^{'} = \frac{\rho}{\rho_0} \ , \quad p^{'} = \frac{p}{p_0} \ , \quad x^{'} = \frac{x}{L} \ , \quad y^{'} = \frac{y}{L}, \quad a_0 = \sqrt{\gamma R T_0} \ ,$$

$$u^{'} = \frac{u}{a_0} , \quad v^{'} = \frac{v}{a_0} , \quad t^{'} = \frac{t}{L \big/ a_0} \qquad (2.11)$$

where, T_0, ρ_0, p_0, are the total or stagnation temperature, density, and pressure, a_0 speed of sound at stagnation condition

After non-dimensionalising ,the 2D Euler equations becomes

$$\frac{\partial w^{'}}{\partial t^{'}} + \frac{\partial f^{'}}{\partial x^{'}} + \frac{\partial g^{'}}{\partial y^{'}} = 0 \qquad (2.12)$$

where,

$$w^{'} = \begin{Bmatrix} \rho^{'} \\ \rho^{'} u^{'} \\ \rho^{'} v^{'} \\ \rho^{'} \left(\dfrac{e^{'}}{\gamma - 1} + \gamma \dfrac{u^{'2} + v^{'2}}{2} \right) \end{Bmatrix} \qquad f^{'} = \begin{Bmatrix} \rho^{'} u^{'} \\ \rho^{'} u^{'2} + \dfrac{p^{'}}{\gamma} \\ \rho^{'} u^{'} v^{'} \\ \rho^{'} \left(\dfrac{e^{'}}{\gamma - 1} + \gamma \dfrac{u^{'2} + v^{'2}}{2} \right) u^{'} + p^{'} u^{'} \end{Bmatrix}$$

$$g^{'} = \begin{Bmatrix} \rho^{'} v^{'} \\ \rho^{'} u^{'} v^{'} \\ \rho^{'} v^{'2} + \dfrac{p^{'}}{\gamma} \\ \rho^{'} \left(\dfrac{e^{'}}{\gamma - 1} + \gamma \dfrac{u^{'2} + v^{'2}}{2} \right) v^{'} + p^{'} v^{'} \end{Bmatrix} \qquad (2.13)$$

By integrating equations (2.12-2.13) over a control volume and applying the Gauss Divergence theorem, the two dimensional Euler equations becomes

8

$$\frac{\partial}{\partial t'}\int_V \rho' dV + \int_s \left[(\rho' u')\vec{i} + (\rho' v')\vec{j}\right] \cdot d\vec{S} = 0 \qquad (2.14)$$

$$\frac{\partial}{\partial t'}\int_V \rho' u' dV + \int_s \left[\left(\rho' u'^2 + \frac{p'}{\gamma}\right)\vec{i} + (\rho' u' v')\vec{j}\right] \cdot d\vec{S} = 0 \qquad (2.15)$$

$$\frac{\partial}{\partial t'}\int_V \rho' v' dV + \int_s \left[(\rho' u' v')\vec{i} + \left(\rho' v'^2 + \frac{p'}{\gamma}\right)\vec{j}\right] \cdot d\vec{S} = 0 \qquad (2.16)$$

$$\frac{\partial}{\partial t'}\int_V \rho' E' dV + \int_s \left[(\rho' E' u' + p' u')\vec{i} + (\rho' E' v' + p' v')\vec{j}\right] \cdot d\vec{S} = 0 \qquad (2.17)$$

Where V indicates volume integral over control volume and S indicates surface integral over surface integral over surface which encloses the control volume.

Here fluxes are represented in terms of the conservative variables as follows,

$$w_1 = \rho' \qquad w_2 = \rho' u' \qquad w_3 = \rho' v' \qquad w_4 = \rho'\left(\frac{e'}{\gamma-1} + \frac{\gamma}{2}\left(\frac{u'^2 + v'^2}{2}\right)\right)$$

$$f_1 = \rho' u' = w_2 \qquad\qquad\qquad g_1 = \rho' v' = w_3$$

$$f_2 = \rho' u'^2 + \frac{1}{\gamma}p' = \frac{w_2^2}{w_1} + \frac{\gamma-1}{\gamma}\left(w_4 - \frac{\gamma}{2}\left(\frac{w_2^2 + w_3^2}{w_1}\right)\right), \quad g_2 = \rho' v' u' = \frac{w_2 w_3}{w_1}$$

$$f_3 = \rho' u' v' = \frac{w_2 w_3}{w_1}, \quad g_3 = \rho' v'^2 + \frac{1}{\gamma}p' = \frac{w_3^2}{w_1} + \frac{\gamma-1}{\gamma}\left(w_4 - \frac{\gamma}{2}\left(\frac{w_2^2 + w_3^2}{w_1}\right)\right)$$

$$f_4 = \rho'\left(\frac{e'}{\gamma-1} + \frac{\gamma}{2}(u'^2 + v'^2)\right)u' + p' u' = \gamma\frac{w_2 w_4}{w_1} - \frac{\gamma(\gamma-1)}{2}w_2\left[\left(\frac{w_2}{w_1}\right)^2 + \left(\frac{w_3}{w_1}\right)^2\right]$$

$$g_4 = \rho'\left(\frac{e'}{\gamma-1} + \frac{\gamma}{2}(u'^2 + v'^2)\right)v' + p' v' = \gamma\frac{w_3 w_4}{w_1} - \frac{\gamma(\gamma-1)}{2}w_3\left[\left(\frac{w_2}{w_1}\right)^2 + \left(\frac{w_3}{w_1}\right)^2\right]$$

2.4.1 Finite Volume Discretization:-

We consider finite volume as shown below in Fig.2.1
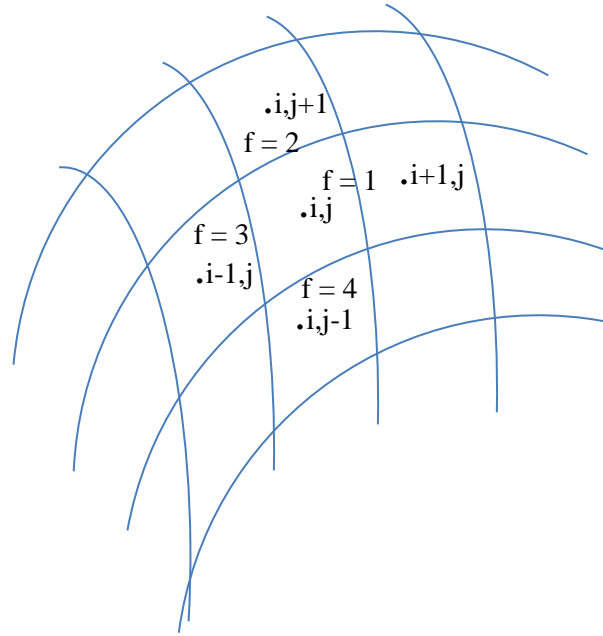
Figure 2.1 Finite volume grid

Predictor step:-

Here the Euler equation in terms of convective fluxes defined as above can be represented as follows,

$$\Delta V \frac{\partial \rho^{'}}{\partial t^{'}} + \sum_{f=1}^{4} \left[(f_1)^n S_{fx} + (g_1)^n S_{fy} \right] = 0 \tag{2.19}$$

$$\Delta V \frac{\partial \rho^{'} u^{'}}{\partial t^{'}} + \sum_{f=1}^{4} \left[(f_2)^n S_{fx} + (g_2)^n S_{fy} \right] = 0 \tag{2.20}$$

$$\Delta V \frac{\partial \rho^{'} v^{'}}{\partial t^{'}} + \sum_{f=1}^{4} \left[(f_3)^n S_{fx} + (g_3)^n S_{fy} \right] = 0 \tag{2.21}$$

$$\Delta V \frac{\partial \rho^{'} E^{'}}{\partial t^{'}} + \sum_{f=1}^{4} \left[(f_4)^n S_{fx} + (g_4)^n S_{fy} \right] = 0 \tag{2.22}$$

All above equations in generalized conservative variable and flux form can be represented as

10

$$\Delta V \frac{\partial w}{\partial t} + \sum_{f=1}^{4} F_f = 0 \qquad (2.23)$$

In the predictor step, fluxes are "forward-differenced" for each face as follows,

$$F_{face1} = f_{i+1,j} S_{fx1} + g_{i+1,j} S_{fy1}$$

$$F_{face2} = f_{i,j+1} S_{fx2} + g_{i,j+1} S_{fy2}$$

$$F_{face3} = f_{i,j} S_{fx3} + g_{i,j} S_{fy3}$$

$$F_{face4} = f_{i,j} S_{fx4} + g_{i,j} S_{fy4} \qquad \ldots\ldots\ldots\ldots (2.24)$$

and the predicted conservative variables are evaluated by,

$$w_{i,j}{}^{p} = w_{i,j}{}^{n} + \left(\frac{\partial w}{\partial t}\right)_{i,j} \Delta t$$

Corrector step:-

Here the general form of the FVM equation

$$\Delta V \frac{\overline{\partial w}}{\partial t} + \sum_{f=1}^{4} F^{p}{}_{f} = 0$$

Predicted conservative variables from predictor step are used to calculate the predicted fluxes and by making use of these fluxes calculate corrected conservative variables as follows,

$$\Delta V \frac{\overline{\partial \rho^{'}}}{\partial t^{'}} + \sum_{f=1}^{4} \left[(f_1)^p S_{fx} + (g_1)^p S_{fy}\right] = 0 \qquad (2.25)$$

$$\Delta V \frac{\overline{\partial \rho^{'} u^{'}}}{\partial t^{'}} + \sum_{f=1}^{4} \left[(f_2)^p S_{fx} + (g_2)^p S_{fy}\right] = 0 \qquad (2.26)$$

$$\Delta V \overline{\frac{\partial \rho' v'}{\partial t'}} + \sum_{f=1}^{4} \left[(f_3)^p S_{fx} + (g_3)^p S_{fy} \right] = 0 \qquad (2.27)$$

$$\Delta V \overline{\frac{\partial \rho' E'}{\partial t'}} + \sum_{f=1}^{4} \left[(f_4)^p S_{fx} + (g_4)^p S_{fy} \right] = 0 \qquad (2.28)$$

In corrector step convective fluxes are "backward-differenced" for each face as follows,

$$F_1^p = f_{i,j}^p S_{fx1} + g_{i,j}^p S_{fy1}$$

$$F_2^p = f_{i,j}^p S_{fx2} + g_{i,j}^p S_{fy2}$$

$$F_3^p = f_{i-1,j}^p S_{fx3} + g_{i-1,j}^p S_{fy3}$$

$$F_4^p = f_{i,j-1}^p S_{fx4} + g_{i,j-1}^p S_{fy4} \qquad \ldots\ldots\ldots\ldots (2.29)$$

So corrected new time step variables are given by,

$$w_{i,j}^{n+1} = w_{i,j}^n + \frac{1}{2} \left[\left(\frac{\partial w}{\partial t} \right)_{i,j} + \left(\overline{\frac{\partial w}{\partial t}} \right)_{i,j} \right] \Delta t$$

2.4.2 Algorithm:-

1. Calculate convective fluxes.

2. Predictor step:-

Solve the set of equations (2.19-2.22) given in the predictor step by "forward-differencing" convective fluxes for each cell face as represented in the set of equations (2.24)

3. Corrector step:-

From the obtained predicted conservative variables values update the predicted fluxes and use these predicted fluxes to calculate corrected conservative variable values by making use of equations (2.25-2.28). Convective fluxes are "backward-differenced" as given in the equations (2.29)

4. New time step conservative variables are updated as follows,

$$w_{i,j}^{n+1} = w_{i,j}^n + \frac{1}{2} \left[\left(\frac{\partial w}{\partial t} \right)_{i,j} + \left(\overline{\frac{\partial w}{\partial t}} \right)_{i,j} \right] \Delta t$$

5. Update new time step conservative variable to old one and also update old convective fluxes.

6. Time step by repeating from 1 to 5 till steady state is reached.

2.5   Variant MacCormack Scheme

By integrating equations (2.12-2.13) over a control volume and applying Gauss Divergence theorem, the two dimensional Euler equation becomes,

$$\frac{\partial}{\partial t'}\int_V \rho' \, dV + \int_S \rho' \vec{u}' \cdot d\vec{S} = 0 \tag{2.30}$$

$$\frac{\partial}{\partial t'}\int_V \rho' u' \, dV + \int_S \rho' u' \left(\vec{u}' \cdot d\vec{S}\right) + \frac{1}{\gamma}\int_S p' \cdot dS_x = 0 \tag{2.31}$$

$$\frac{\partial}{\partial t'}\int_V \rho' v' \, dV + \int_S \rho' v' \left(\vec{u}' \cdot d\vec{S}\right) + \frac{1}{\gamma}\int_S p' \cdot dS_y = 0 \tag{2.32}$$

$$\frac{\partial}{\partial t'}\int_V \rho' E' \, dV + \int_S \rho' E' \left(\vec{u}' \cdot d\vec{S}\right) + \int_S p' \left(\vec{u}' \cdot d\vec{S}\right) = 0 \tag{2.33}$$

2.5.1   Volume flux:-

The outward volume flux, F_f, through the face f, is defined by

$$F_f \equiv \int_{S_f} \vec{u}'_f \cdot d\vec{S}_f$$

where, $d\vec{S}_f$ is the differential element on the area of the fth cell face and $\vec{u}'_f$ is the velocity defined at the face f. We assume that,

$$F_f = \vec{u}'_f \cdot \vec{S}_f$$

where, $\vec{u}'_f$ is now the velocity at the face center and $\vec{S}_f$ is the total (outward) surface vector of face f.

13

However we can conceive of a variant MacCormack scheme, where the fluxes F_f are not forward or backward differenced but are center differenced for both predictor and corrector steps. This approach is similar to that done in incompressible flows. However the conservative variables $\rho^{'}, \rho^{'}u^{'}, \rho^{'}v^{'}, \rho^{'}E^{'}$ and the pressure $p^{'}$ will be forward and backward differenced for predictor and corrector step respectively, as used. This alternate scheme we will hitherto refer as the "variant MacCormack scheme".

2.5.2   Finite Volume Discretization :-

1. Predictor step:-

$$\Delta V \frac{\partial \rho^{'}}{\partial t^{'}} + \sum_{f=1}^{4} \rho_{f}^{'n} F_{f}^{n} = 0 \qquad (2.34)$$

$$\Delta V \frac{\partial \rho^{'}u^{'}}{\partial t^{'}} + \sum_{f=1}^{4} \left(\rho^{'}u^{'}\right)_{f}^{n} F_{f}^{n} + \frac{1}{\gamma}\sum_{f=1}^{4} p_{f}^{n} S_{fx} = 0 \qquad (2.35)$$

$$\Delta V \frac{\partial \rho^{'}v^{'}}{\partial t^{'}} + \sum_{f=1}^{4} \left(\rho^{'}v^{'}\right)_{f}^{n} F_{f}^{n} + \frac{1}{\gamma}\sum_{f=1}^{4} p_{f}^{n} S_{fy} = 0 \qquad (2.36)$$

$$\Delta V \frac{\partial \rho^{'}E^{'}}{\partial t^{'}} + \sum_{f=1}^{4} \left(\rho^{'}E^{'}\right)_{f}^{n} F_{f}^{n} + \sum_{f=1}^{4} p_{f}^{n} F_{f}^{n} = 0 \qquad (2.37)$$

Here all the convective and pressure terms are "forward-differenced" and volume flux as explained above is center differenced.

Predicted conservative values are given by,

$$w_{i,j}^{p} = w_{i,j}^{n} + \left(\frac{\partial w}{\partial t}\right)_{i,j} \Delta t$$

2. Corrector step:-

Predicted conservative variables are used to calculate corrected values

$$\Delta V \frac{\overline{\partial \rho^{'}}}{\partial t} + \sum_{f=1}^{4} \rho_{f}^{'p} F_{f}^{p} = 0 \qquad (2.38)$$

$$\Delta v \overline{\frac{\partial \rho' u'}{\partial t'}} + \sum_{f=1}^{4}\left(\rho' u'\right)_f^p F_f^p + \frac{1}{\gamma}\sum_{f=1}^{4} p_f^p S_{fx} = 0 \qquad (2.39)$$

$$\Delta v \overline{\frac{\partial \rho' v'}{\partial t'}} + \sum_{f=1}^{4}\left(\rho' v'\right)_f^p F_f^p + \frac{1}{\gamma}\sum_{f=1}^{4} p_f^p S_{fy} = 0 \qquad (2.40)$$

$$\Delta v \overline{\frac{\partial \rho' E'}{\partial t'}} + \sum_{f=1}^{4}\left(\rho' E'\right)_f^p F_f^p + \sum_{f=1}^{4} p_f^p F_f^p = 0 \qquad (2.41)$$

Here convective and pressure terms are "backward-differenced"

Similar to predictor step temporal term for corrector step as follows,

$$w_{i,j}^{n+1} = w_{i,j}^{n} + \frac{1}{2}\left[\left(\frac{\partial w}{\partial t}\right)_{i,j} + \left(\overline{\frac{\partial w}{\partial t}}\right)_{i,j}\right]\Delta t$$

$$(2.28)$$

2.5.3   Algorithm:-

1. Calculate volume fluxes.

2. Predictor step:-

Solve the set of equations given in the predictor step. Conservative variables and pressure at the face centers f =1, 2, 3, 4 are "forward-differenced" as follows.

$$W_1 = W_{i+1,j}, W_2 = W_{i,j+1}, W_3 = W_{i,j}, W_4 = W_{i,j}$$

$$P_1 = P_{i+1,j}, P_2 = P_{i,j+1}, P_3 = P_{i,j}, P_4 = P_{i,j}$$

3. Corrector step:-

Solve set of equations given in the corrector step by making use of the predicted values. Conservative variables and pressure in the corrector step at the face center f=1,2,3,4 are "backward-differenced" as follows ,

$$W_1 = W_2 = W_{i,j}^p, W_3 = W_{i-1,j}^p, W_4 = W_{i,j-1}^p$$

$$p_1^p = p_2^p = p_{i,j}^p, p_3^p = p_{i-1,j}^p, p_4^p = p_{i,j-1}^p$$

15

4. New time step conservative variables are updated as follows,

$$w_{i,j}^{n+1} = w_{i,j}^{n} + \frac{1}{2}\left[\left(\frac{\partial w}{\partial t}\right)_{i,j} + \left(\overline{\frac{\partial w}{\partial t}}\right)_{i,j}\right]\Delta t$$

5. Update new time step conservative variable to old one.

6. Time step by repeating from 1 to 5 till steady state is reached.

2.5.4   Artificial Viscosity addition to MacCormack by Jameson's method :-

As explained earlier in section 2.2 the Euler equations require some artificial viscosity in order have stability and smoothing of the solution. Adding viscosity also helps in rapid convergence towards the solution.

Here artificial viscosity is added in the predictor and corrector step as follows,

1. Predictor step:-

$$w_{i,j}^{p} = w_{i,j}^{n} + \left(\frac{\partial w}{\partial t}\right)_{i,j}\Delta t + AD\left(w_{i,j}\right)^{n}$$

Where $AD(w_{i,j})^{n}$ is artificial viscosity which is given by,

$$AD\left(w_{i,j}\right)^{n} = C_{x}\gamma_{1}\left(w_{i+1,j}^{n} - 2w_{i,j}^{n} + w_{i-1,j}^{n}\right) + C_{y}\gamma_{2}\left(w_{i,j+1}^{n} - 2w_{i,j}^{n} + w_{i,j-1}^{n}\right) \quad (2.29)$$

C_{x} and C_{y} are constants, values of these constants can be chosen between 0 to 1.

$$\gamma_{1} = \frac{\left|p_{i+1,j}^{n} - 2p_{i,j}^{n} + p_{i-1,j}^{n}\right|}{\left|p_{i+1,j}^{n}\right| + 2\left|p_{i,j}^{n}\right| + \left|p_{i-1,j}^{n}\right|} \quad \text{and} \quad \gamma_{2} = \frac{\left|p_{i,j+1}^{n} - 2p_{i,j}^{n} + p_{i,j-1}^{n}\right|}{\left|p_{i,j+1}^{n}\right| + 2\left|p_{i,j}^{n}\right| + \left|p_{i,j-1}^{n}\right|} \quad (2.30)$$

2. Corrector step:-

$$w_{i,j}^{n+1} = w_{i,j}^{n} + \frac{1}{2}\left(\frac{\partial w}{\partial t} + \overline{\frac{\partial w}{\partial t}}\right)\Delta t + AD\left(w_{i,j}\right)^{p}$$

16

$$AD\left(w_{i,j}\right)^P = C_x \gamma_1 \left(w_{i+1,j}^p - 2w_{i,j}^p + w_{i-1,j}^p\right) + C_y \gamma_2 \left(w_{i,j+1}^p - 2w_{i,j}^p + w_{i,j-1}^p\right) \quad (2.31)$$

$$\gamma_1 = \frac{\left|p_{i+1,j}^p - 2p_{i,j}^p + p_{i-1,j}^p\right|}{\left|p_{i+1,j}^p\right| + 2\left|p_{i,j}^p\right| + \left|p_{i-1,j}^p\right|} \quad \text{and} \quad \gamma_2 = \frac{\left|p_{i,j+1}^p - 2p_{i,j}^p + p_{i,j-1}^p\right|}{\left|p_{i,j+1}^p\right| + 2\left|p_{i,j}^p\right| + \left|p_{i,j-1}^p\right|} \quad (2.32)$$

Pressure and conservative variables used to calculate artificial viscosity in corrector step are predicted values of pressure and conservative variables. Since the artificial dissipation term is of third order, the overall accuracy of the scheme is of second order. The stability condition of the scheme limits the time step.

$$\Delta t \leq CFL \left(\frac{\left|u_{max}\right| + a}{\Delta x_{min}} + \frac{\left|v_{max}\right| + a}{\Delta y_{min}}\right)^{-1} \quad (2.33)$$

where a denotes the local speed of sound, umax and v max are the maximum velocities in the domain, and *CFL < 1*.

2.6 Total Variation Diminishing (TVD) schemes:-

Numerical schemes of second and even higher orders of accuracy have oscillatory behavior. This oscillatory behavior creates errors in the solution, which can lead to non-physical values of quantities which are physically bounded. Godunov (1959) introduced an important concept known as 'monotonicity' to characterize numerical schemes. Monotonicity means no new extrema should be created other than extremas which are already present in the initial solution. That is the maxima in the solution must be non-increasing and minima non-decreasing. Oscillating solutions are non-monotonic. For non-linear equations Harten (1983-1984) the concept of bounded total variation and the Total Variation Diminishing criteria. The principal condition of TVD schemes is that the total variation of the solution, defined as

$$TV = \sum_I \left|U_{I+1} - U_I\right|$$

for a scalar conservation equation ,should decrease with time. The TVD property ensures that unwanted oscillations are not generated in the solution and monotonicity is preserved,

which allows strong shock waves to be accurately captured without any spurious oscillations of the solution. In TVD schemes limiters or limiter functions prevent unwanted spurious solutions in the region of high gradient. Limiters maintain the original higher order discretization of the numerical scheme in the smooth flow regions, but in the regions of high gradients and /or strong discontinuities the limiter has to reduce the order of the thereby adding high numerical dissipation to prevent the generation of spurious extrema.

2.6.1 TVD-MacCormack scheme :-

This Modified Causon's scheme is based on the classical MacCormack FVM scheme in total variation diminishing (TVD) form, which is also known as Modified Causon's scheme[18].

This scheme has the following three steps of which the first two are the classical MacCormack predictor-corrector steps:

1. Predictor step:-

$$w_{i,j}^{p} = w_{i,j}^{n} + \left(\frac{\partial w}{\partial t} \right)_{i,j} \Delta t$$

2. Corrector step:-

$$\overline{w_{i,j}^{n+1}} = w_{i,j}^{n} + \frac{1}{2} \left(\frac{\partial w}{\partial t} + \frac{\overline{\partial w}}{\partial t} \right) \Delta t$$

3. Addition of artificial viscosity by TVD:-

$$w_{i,j}^{n+1} = \overline{w_{i,j}^{n+1}} + {}^{(TVD)}w_{i,j}^{1n} + {}^{(TVD)}w_{i,j}^{2n} \tag{2.33}$$

Where $(W_{i,j})^{n+1}$ is the corrected numerical solution at $(n+1)^{th}$ time level.

Second term in (2.33) is one-dimensional TVD-type viscosity term in the direction of the change of index i in step 3 equation, proposed by Causon, is given by

$${}^{(TVD)}w_{i,j}^{1n} = \lfloor P_{i,j}^{+} + P_{i+1,j}^{-} \rfloor (w_{i+1,j}^{n} - w_{i,j}^{n}) - \lfloor P_{i-1,j}^{+} + P_{i,j}^{-} \rfloor (w_{i,j}^{n} - w_{i-1,j}^{n}) \tag{2.34}$$

$$P_{i,j}^{\pm} \equiv P(r_{i,j}^{\pm}) = \frac{1}{2} C(v_{i,j}) [1 - \phi(r_{i,j}^{\pm})] \tag{2.35}$$

$$r_{i,j}^{+} = \frac{\left(w_{i+1,j}^{n} - w_{i,j}^{n}, w_{i,j}^{n} - w_{i-1,j}^{n}\right)}{\left(w_{i+1,j}^{n} - w_{i,j}^{n}, w_{i+1,j}^{n} - w_{i,j}^{n}\right)} \qquad , \qquad r_{i,j}^{-} = \frac{\left(w_{i+1,j}^{n} - w_{i,j}^{n}, w_{i,j}^{n} - w_{i-1,j}^{n}\right)}{\left(w_{i,j}^{n} - w_{i-1,j}^{n}, w_{i,j}^{n} - w_{i-1,j}^{n}\right)}$$

In these relations $(\cdot, \cdot)$ denotes the scalar product of two vectors. The flux limiter $\Phi(r_{ij}^{\pm})$ and the function $C(v_{i,j})$ in relation (2.35) are defined as.

$$\emptyset(r_{i,j}^{\pm}) = \begin{cases} min(2r_{i,j}^{\pm}, 1) & for\ r_{i,j}^{\pm} > 0 \\ 0 & for\ r_{i,j}^{\pm} \le 0 \end{cases} \quad , C(v_{i,j}) = \begin{cases} v_{i,j}(1 - v_{i,j}) & for\ v_{i,j} \le \frac{1}{2} \\ 0.25 & for\ v_{i,j} > \frac{1}{2} \end{cases}$$

$$\dots (2.36)$$

And $v_{i,j}$ is given by the following formula

$$v_{i,j} = \frac{\Delta t}{\Delta x_{i,j}} \left(|u_{i,j}| + a_{i,j}\right) \tag{2.37}$$

Where, $u_{i,j}$ is the velocity in x-direction and $a_{i,j}$ is the local speed of sound.

In a similar manner artificial viscosity in the j direction is also added $^{(TVD)}W_{i,j}^{2n}$.

2.7   Semi-implicit MacCormack scheme:-

The schemes discussed above are all explicit. We will now introduce a semi-implicit scheme based on the variant MacCormack scheme.

All equations given below are solved by semi-implicit method. Here the variables for which we are solving are considered at   predictor time level and $(n+1/2)^{th}$ time level for predictor and corrector step respectively and remaining quantities such as volume flux, pressure are considered at n^{th} level . Finite volume discretization of the equations in semi-implicit form is as follows.

1. Predictor step:-

$$\Delta V \frac{\rho_{i,j}^{'p} - \rho_{i,j}^{'n}}{\Delta t^{'}} + \sum_{f=1}^{4} \rho_{f}^{'p} F_{f}^{n} = 0 \tag{2.38}$$

$$\Delta V \frac{(\rho^{'}u^{'})_{i,j}^{p} - (\rho^{'}u^{'})_{i,j}^{n}}{\Delta t^{'}} + \sum_{f=1}^{4} (\rho^{'}u^{'})_{f}^{p} F_{f}^{n} + \frac{1}{\gamma} \sum_{f=1}^{4} p_{f}^{n} S_{fx} = 0 \tag{2.39}$$

$$\Delta V \frac{\left(\rho' v'\right)_{i,j}^{p} - \left(\rho' v'\right)_{i,j}^{n}}{\Delta t'} + \sum_{f=1}^{4}\left(\rho' v'\right)_{f}^{p} F_{f}^{n} + \frac{1}{\gamma}\sum_{f=1}^{4} p_{f}^{n} S_{fy} = 0 \qquad (2.40)$$

$$\Delta V \frac{\left(\rho' E'\right)_{i,j}^{p} - \left(\rho' E'\right)_{i,j}^{n}}{\Delta t'} + \sum_{f=1}^{4}\left(\rho' E'\right)_{f}^{p} F_{f}^{n} + \sum_{f=1}^{4} p_{f}^{n} F_{f}^{n} = 0 \qquad (2.41)$$

Conservative variables on the face centers can be taken by forward differencing as follows,

$$w_{1} = w_{i+1,j}^{p}, w_{2} = w_{i,j+1}^{p}, w_{3} = w_{4} = w_{i,j}^{p}$$

Then above equations are solved semi-implicitly by Gauss-Seidel loop to get the predicted values at the Pth level.

2. Corrector step:-

Predicted conservative variables obtained from predictor step are used in this step in order to calculate conservative variables at $(n+1/2)^{th}$ level .While for volume flux velocity components used are from n^{th} time level.

$$\Delta V \frac{\rho_{i,j}^{'n+\frac{1}{2}} - \rho_{i,j}^{'n}}{\Delta t'} + \sum_{f=1}^{4} \rho_{i,j}^{'n+\frac{1}{2}} F_{f}^{p} = 0 \qquad (2.42)$$

$$\Delta V \frac{\left(\rho' u'\right)_{i,j}^{n+\frac{1}{2}} - \left(\rho' u'\right)_{i,j}^{n}}{\Delta t'} + \sum_{f=1}^{4}\left(\rho' u'\right)_{f}^{n+\frac{1}{2}} F_{f}^{p} + \frac{1}{\gamma}\sum_{f=1}^{4} p_{f}^{n} S_{fx} = 0 \qquad (2.43)$$

$$\Delta V \frac{\left(\rho' v'\right)_{i,j}^{n+\frac{1}{2}} - \left(\rho' v'\right)_{i,j}^{n}}{\Delta t'} + \sum_{f=1}^{4}\left(\rho' v'\right)_{f}^{n+\frac{1}{2}} F_{f}^{p} + \frac{1}{\gamma}\sum_{f=1}^{4} p_{f}^{n} S_{fy} = 0 \qquad (2.44)$$

$$\Delta V \frac{\left(\rho' E'\right)_{i,j}^{n+\frac{1}{2}} - \left(\rho' E'\right)_{i,j}^{n}}{\Delta t'} + \sum_{f=1}^{4}\left(\rho' E'\right)_{f}^{n+\frac{1}{2}} F_{f}^{p} + \sum_{f=1}^{4} p_{f}^{n} F_{f}^{p} = 0 \qquad (2.45)$$

Conservative variables on the face centers are backward differenced as follows

$$w_{1} = w_{i-1,j}^{n+\frac{1}{2}}, w_{2} = w_{i,j-1}^{n+\frac{1}{2}}, w_{3} = w_{4} = w_{i,j}^{n+\frac{1}{2}}$$

So in the similar manner as in the predictor step equations are solved for $(n+1/2)^{th}$ level semi-implicitly by Gauss-Seidel loop.

Then the new time step conservative variable can be calculated as follows

$$w_{i,j}^{n+1} = \frac{1}{2}\left(w_{i,j}^{p} + w_{i,j}^{n+\frac{1}{2}}\right)$$

Then update variables and time step it till steady state.

2.8   Boundary Conditions:-

For a physical problem to be solvable it has to be "well-posed", which means that the solution should be unique and stable and depend continuously on the boundary and initial conditions. The boundary conditions provided should be such that this type of solution is obtained. The boundary conditions that determines the well-posedne of a general partial differential equation is not easy to determine.

In literature different mathematical theories of boundary conditions have been discussed. Kreiss [19] developed one dimensional theory of boundary conditions for according to the incoming characteristics into the domain. Similar approach is discussed by Whitefield and Janus [20]. Other researchers like Rudy and Strikwerda[21], Gustafson[22], Dutt[23], Oliger and Sundstrom[24]   also developed mathematical theories of boundary conditions. Euler equations are hyperbolic in nature so information passes in one (left or right) or two directions (left and right) depending upon the flow regimes at inlet and outlet. In order to understand boundary conditions for compressible flow consider the one dimensional Euler equation.

$$\frac{\partial U}{\partial t} + \frac{\partial F}{\partial x} = 0 \qquad \text{Or} \qquad \frac{\partial U}{\partial t} + A\frac{\partial U}{\partial x} = 0 \qquad (2.46)$$

where,

$$A = \frac{\partial F}{\partial U}$$

Equation (2.46) is hyperbolic if and only if matrix A is diagonalizable.

$$Q^{-1}AQ = D \qquad (2.47)$$

where D is a diagonal matrix whose diagonal elements are characteristic values or eigenvalues of A. Q is a matrix whose columns are right characteristic vectors or right eigenvectors of A, and Q^{-1} is a matrix whose rows are left characteristic vectors or left eigenvectors of A. These Eigen values are the characteristic variables or Riemann invariants in one dimension.

Multiply both sides of equation (2.46) by Q^{-1}

$$Q^{-1}\frac{\partial U}{\partial t} + Q^{-1}A\frac{\partial U}{\partial x} = 0 \qquad (2.48)$$

and define $\quad \partial v = Q^{-1}\partial U \qquad$ and $\qquad \partial U = Q\partial v$

$$\frac{\partial v}{\partial t} + D\frac{\partial v}{\partial x} = 0 \qquad (2.49)$$

Equation (2.49) is the characteristic form of the governing equation. If we consider the characteristic form of Euler equation then

$$D = \begin{bmatrix} u & & \\ & u+a & \\ & & u-a \end{bmatrix} \qquad (2.50)$$

The general rule is that the number of positive eigenvalues at a *left* boundary is the number ("Dirichlett –type ") boundary conditions, called "physical boundary conditions" ,while the number of negative eigenvalues gives the number of "numerical boundary conditions", based on extrapolation from the flow field, that will have to be used. On a *right* boundary, the positive eigenvalues give the number of the numerical boundary conditions, while the negative eigenvalues give the physical boundary conditions required. For the case of Euler equation, this is shown in the Figure (2.8). The details of the conservative variables of the Euler equations are given in Table 2.8
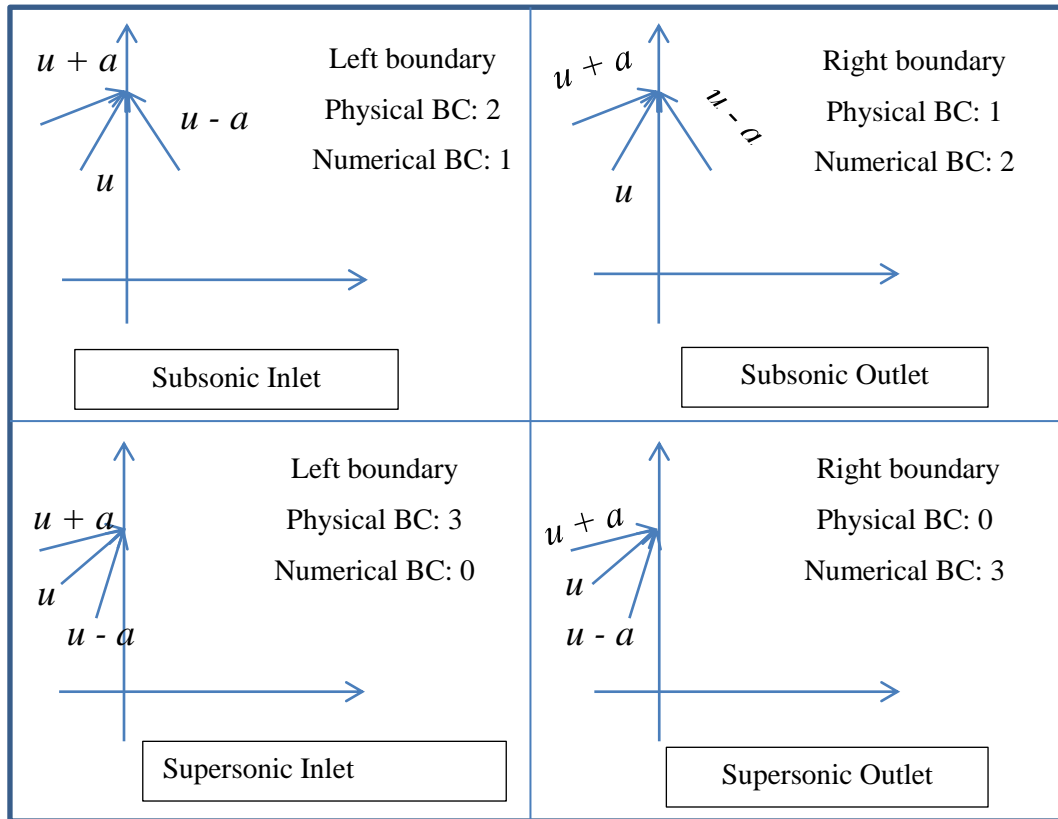
Figure 2.2 Speed regimes and characteristic variables entering and leaving domain.

Table 2.1 Boundary Conditions tables

	1 D		2D		3D	
	Physical	Numerical	Physical	Numerical	Physical	Numerical
Subsonic Inflow	ρ, ρE	ρV	ρ, ρE	ρV_i	ρ, ρE	ρV_i
Subsonic Outflow	ρV or Pressure ratio	All other variables are extrapolated	ρV_i or Pressure ratio	All other variables are extrapolated	ρV_i or Pressure ratio	All other variables are extrapolated
Supersonic Inflow	ρ, ρV, ρE	None	ρ, ρV_i, ρE	None	ρ, ρV_i, ρE	None
Supersonic Outflow	None	ρ, ρV, ρE	None	ρ, ρV_i, ρE	None	ρ, ρV_i, ρE

2.8.1   Inviscid flow over solid boundaries :-

In inviscid flow the fluid slips over solid boundaries. That is there is no flow normal to the surface, so convective fluxes passing through this solid boundary reduces to the pressure term alone.

So the convective terms at the wall are

$$
f_w\left(S_{fx}\right)_1 + g_w\left(S_{fy}\right)_1 = p \left\{ \begin{array}{c} 0 \\ S_{fx} \\ S_{fy} \\ 0 \end{array} \right\}
$$

where, p is evaluated during forward and backward differencing by an interior pressure cell value.

Closure:-

We have discussed here the MacCormack scheme and three variants of the MacCormack. Of the later one scheme introduces artificial viscosity using Jameson's method, the second by TVD concept and the third is a semi-implicit version of the variant MacCormack scheme. These schemes will be used in the following chapters. Boundary conditions are also discussed in this chapter.

Chapter 3

Results and Discussion- 1D Problems

3.1   Mathematical models to check boundary conditions

In order to see the effect of the wave interaction and different boundary conditions in accordance with the speed regimes at the inflow and outflow boundaries. Analytical test cases has been formulated which are similar to the flow conditions like subsonic inlet - subsonic outlet, supersonic inlet – supersonic outlet etc.

3.1.1   First mathematical model

Consider a first order partial differential equation in characteristic form

$$\frac{\partial v}{\partial t} + D \frac{\partial v}{\partial x} = 0$$

Consider a diagnolized matrix D

$$D = \begin{Bmatrix} 1 & & \\ & 2 & \\ & & -1 \end{Bmatrix}$$

Above diagnolized matrix resembles conditions of subsonic inlet and subsonic outlet since two eigenvalues are positive and one eigenvalue is negative. Converting this characteristic form of PDE into conservative form, a simplified version of subsonic inlet and subsonic outflow conditions can be simulated.   In conservative form all three equations will get coupled, like compressible flow Euler equations. We choose Q matrix as

$$Q = \begin{bmatrix} \frac{1}{\sqrt{2}} & 0 & \frac{1}{\sqrt{2}} \\ 0 & 0 & 0 \\ \frac{1}{\sqrt{2}} & 0 & -\frac{1}{\sqrt{2}} \end{bmatrix}$$

$$A = QDQ^{-1} = \begin{bmatrix} 0 & 0 & 1 \\ 0 & 2 & 0 \\ 1 & 0 & 0 \end{bmatrix}$$

So

$$\begin{Bmatrix} u1 \\ u2 \\ u3 \end{Bmatrix} = \begin{bmatrix} \dfrac{1}{\sqrt{2}} & 0 & \dfrac{1}{\sqrt{2}} \\ 0 & 1 & 0 \\ \dfrac{1}{\sqrt{2}} & 0 & -\dfrac{1}{\sqrt{2}} \end{bmatrix} \begin{Bmatrix} v1 \\ v2 \\ v3 \end{Bmatrix}$$

(3.1)

So we will solve these conservative forms of PDE's

$$\frac{\partial}{\partial t} \begin{Bmatrix} u1 \\ u2 \\ u3 \end{Bmatrix} + [A]\frac{\partial}{\partial x} \begin{Bmatrix} u1 \\ u2 \\ u3 \end{Bmatrix} = 0$$

3.1.2 Second mathematical model

This resembles the supersonic inlet and supersonic outlet case. The diagnolized matrix is

$$D = \begin{bmatrix} 1 & & \\ & 2 & \\ & & 1 \end{bmatrix}$$

and the Q matrix is

$$Q = \begin{bmatrix} \dfrac{1}{\sqrt{2}} & \dfrac{1}{2} & \dfrac{1}{2} \\ -\dfrac{1}{\sqrt{2}} & \dfrac{1}{2} & \dfrac{1}{2} \\ 0 & -\dfrac{1}{\sqrt{2}} & \dfrac{1}{\sqrt{2}} \end{bmatrix}$$

Conservative and the characteristic variables are related to each other by

26

$$\begin{Bmatrix} u1 \\ u2 \\ u3 \end{Bmatrix} = \begin{bmatrix} \dfrac{1}{\sqrt{2}} & \dfrac{1}{2} & \dfrac{1}{2} \\[2mm] -\dfrac{1}{\sqrt{2}} & \dfrac{1}{2} & \dfrac{1}{2} \\[2mm] 0 & -\dfrac{1}{\sqrt{2}} & \dfrac{1}{\sqrt{2}} \end{bmatrix} \begin{Bmatrix} v1 \\ v2 \\ v3 \end{Bmatrix} \qquad (3.2)$$

Boundary Conditions:-

For both the problems boundary conditions are specified in characteristic form but while imposing they are imposed in conservative form that is in terms of (u1, u2, and u3) as per the relationship given between variables *u's* and *v's* in equations (3.1) and (3.2)

Variables	Boundary conditions
V1	$\begin{cases} 0 & \text{for } t \le 0 \\[4mm] sint & \text{for } t \ge 0 \end{cases}$
V2	$\begin{cases} 0 & \text{for } t \le 0 \\[4mm] 1 - e^{-t} & \text{for } t \ge 0 \end{cases}$
V3	$\begin{cases} 0 & \text{for } t \le 0 \\[4mm] 1 - cost & \text{for } t \ge 0 \end{cases}$

Here for solving these equations MacCormack scheme is used.

Results for these two problems the numerical and analytical results are as shown below
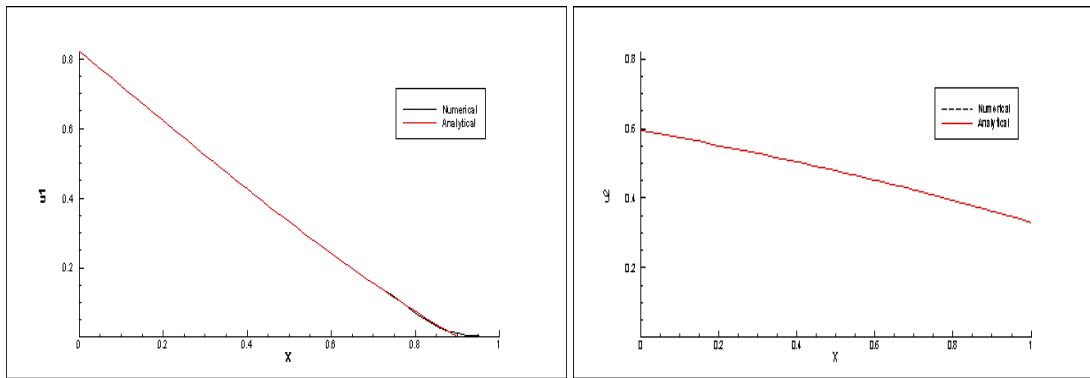
(a)

(b)
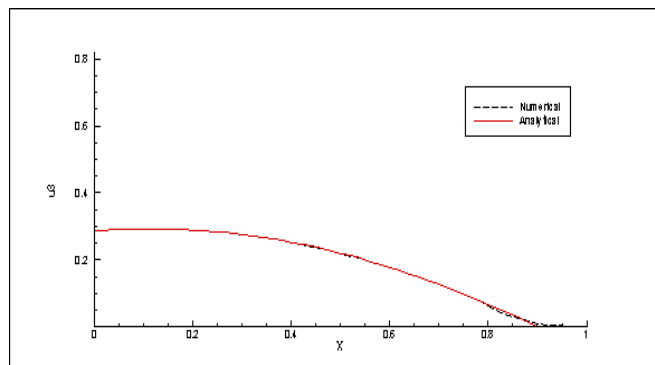
(c)

Fig.3.1 1 Analytical and numerical results of 3.1.1 problem (a) for u1, (b) for u2 and (c) for u3
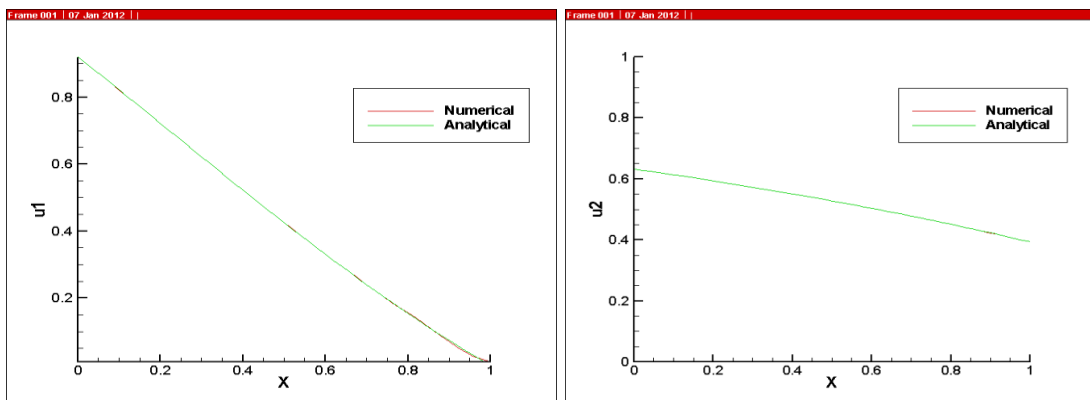
(b)
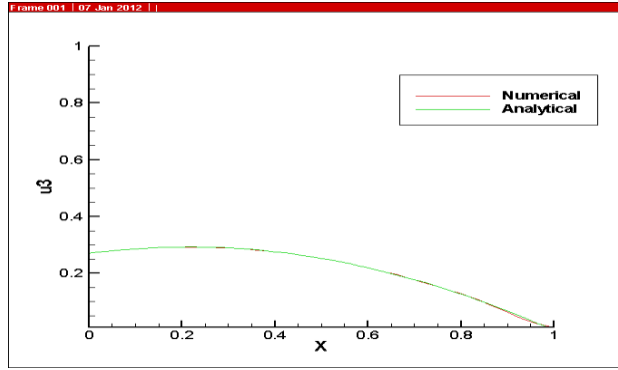
(c)

Fig. 3.1.2 Analytical and numerical results of 3.1.2 problem, (a) for u1, (b) for u2 and (c) for u3

3.2   Quasi one dimensional flows

For a variable area stream tube, the flow field is three dimensional, where the flow properties are functions of *x, y,* and *z*. However if the variation of area *A=A(x)* is gradual, it is often convenient and sufficiently accurate to neglect the *y* and *z* flow variables, and to assume that the flow properties are constant across the flow at every *x* station. Such a flow, where the area varies as *A=A(x)* and where it is assumed that *p, ρ, T,* and *u* are still functions of x only, is called Quasi-one-dimensional flow.

Governing equations for Quasi-one-dimensional flow:-

Continuity Equation

$$\frac{\partial(\rho A)}{\partial t} + \frac{\partial(\rho AV)}{\partial x} = 0 \qquad (3.3)$$

Momentum Equation

$$\frac{\partial(\rho AV)}{\partial t} + \frac{\partial(\rho AV^2 + pA)}{\partial x} = p\frac{\partial A}{\partial x} \qquad (3.4)$$

Energy Equation

$$\frac{\partial\left[\rho\left(e + V^2/2\right)A\right]}{\partial t} + \frac{\partial\left[\rho\left(e + V^2/2\right)AV + pAV\right]}{\partial x} = 0 \qquad (3.5)$$

Above equations are solved in non-dimensionalized form, for these the non-dimensionalized variables are

$$T' = \frac{T}{T_0} \;,\; \rho' = \frac{\rho}{\rho_0} \;,\; p' = \frac{p}{p_0} \;,\; x' = \frac{x}{L} \;,\; a_0 = \sqrt{\gamma R T_0} \;,\; V' = \frac{V}{a_0} \;,\; t' = \frac{t}{L/a_0} \;,\; A' = \frac{A}{A^*}$$

Where, T_0, ρ_0, p_0, are the total or stagnation temperature, density, and pressure, a_0 speed of sound at stagnation condition, V mean speed of flow, L- Length of nozzle, A-Area of nozzle, A^*- Area of nozzle where flow becomes sonic and t is time.

So the non-dimensionalzed governing equations are as follows,

$$\frac{\partial(\rho' A')}{\partial t'} + \frac{\partial(\rho' A' V')}{\partial x'} = 0$$

$$\frac{\partial(\rho' A' V')}{\partial t'} + \frac{\partial\left(\rho' A' V'^2 + \left(1/\gamma\right) p' A'\right)}{\partial x'} = \frac{1}{\gamma} p' \frac{\partial A'}{\partial x'}$$

$$\frac{\partial\left[\rho'\left(\frac{e'}{\gamma-1} + \gamma V'^2/2\right) A'\right]}{\partial t'} + \frac{\partial\left[\rho'\left(\frac{e'}{\gamma-1} + \gamma V'^2/2\right) A' V' + p' A' V'\right]}{\partial x'} = 0$$

Here flux is expressed in terms of conservative variables.

$$U1 = \rho' A' \qquad U2 = \rho' A' V' \qquad U3 = \rho'\left(\frac{e'}{\gamma-1} + \frac{\gamma}{2} V'^2\right) A'$$

$$F_1 = \rho' A' V' = U_2 \qquad F_2 = \rho' A' V'^2 + \frac{1}{\gamma} p' A' = \frac{U_2^2}{U_1} + \frac{\gamma-1}{\gamma}\left(U_3 - \frac{\gamma}{2}\frac{U_2^2}{U_1}\right)$$

$$F_3 = \rho'\left(\frac{e'}{\gamma-1} + \frac{\gamma}{2} V'^2\right) V' A' + p' A' V' = \gamma \frac{U_2 U_3}{U_1} - \frac{\gamma(\gamma-1)}{2}\frac{U_2^3}{U_1^2} \qquad J_2 = \frac{1}{\gamma} p' \frac{\partial A'}{\partial x'} \qquad (3.6)$$

Therefore the above set of equations becomes,

$$\frac{\partial U_1}{\partial t} + \frac{\partial F_1}{\partial x} = 0 \qquad \frac{\partial U_2}{\partial t} + \frac{\partial F_2}{\partial x} = J_2 \qquad \frac{\partial U_3}{\partial t} + \frac{\partial F_3}{\partial x} = 0 \qquad (3.7)$$

,

,

Above equations can be directly discretized for MacCormack scheme in FDM. In order to solve these equations by FVM we have to forward difference or backward difference only the conservative variables for which we are solving.

Table 3.1 Forward and Backward differencing of variables

	FDM	FVM
Variables to be forward and backward differenced	$F_1 = \rho' A' V'$ $F_2 = \rho' A' V'^2 + \dfrac{1}{\gamma} p' A'$ $F_3 = \rho'\left(\dfrac{e'}{\gamma-1} + \dfrac{\gamma}{2} V'^2\right) V' A' + p' A' V'$	ρ' $\rho' u'$ $\rho'\left(\dfrac{e'}{\gamma-1} + \dfrac{\gamma}{2} V'^2\right)$

Problem definition:-

The problems that we are solving here are steady, isentropic flow through convergent-divergent nozzle, and convergent nozzle (for subsonic to subsonic flow without shock case). The flow at the inlet to the nozzle comes from a reservoir where the pressure and temperature are denoted by P_0 and T_0, respectively. Thus P_0 and T_0 are the stagnation values, or total pressure and total temperature values. First case will be the subsonic flow to supersonic flow, second case is subsonic flow to subsonic flow without shock, and third one is subsonic flow to subsonic flow with shock.

Table 3.2 Areas of nozzle for different cases

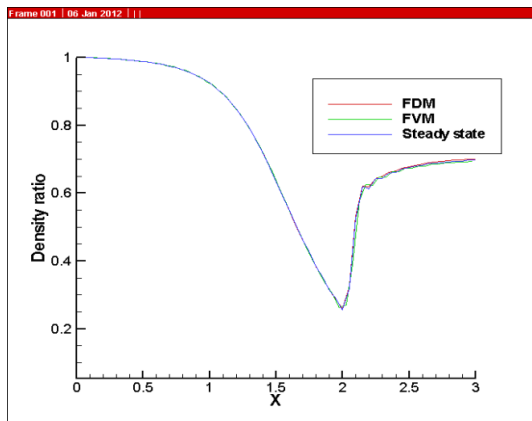| Subsonic-Supersonic flow (Convergent-Divergent (CD) nozzle)	Subsonic-subsonic without shock(convergent nozzle)	Subsonic to subsonic with shock(CD-nozzle)
$A = 1 + 2.2(x-1.5)^2 \quad 0 \le x \le 3$	$\dfrac{A}{A_t} = 1 + 2.2\left(\dfrac{x}{L} - 1.5\right)^2 \quad 0 \le \dfrac{x}{L} \le 1.5$ $\dfrac{A}{A_t} = 1 + 0.2223\left(\dfrac{x}{L} - 1.5\right)^2 \quad 1.5 \le \dfrac{x}{L} \le 3$	$A = 1 + 2.2(x-1.5)^2$ $0 \le x \le 3$

3.2.1   Subsonic-Supersonic flow

Initial Conditions:-

Table 3.3 Initial conditions for subsonic to supersonic flow

Distance	$0 \leq x \leq 0.5$	$0.5 \leq x \leq 1.5$	$1.5 \leq x \leq 3$
ρ	1	$1 - 0.366\left(x^{'} - 0.5\right)$	$0.634 - 0.3879\left(x^{'} - 1.5\right)$
T	1	$1 - 0.167\left(x^{'} - 0.5\right)$	$0.833 - 0.3507\left(x^{'} - 1.5\right)$
ρv		0.59	

Boundary conditions:-

Table 3.4 Boundary conditions for subsonic to supersonic flow

Subsonic inlet	Supersonic outlet
$\dfrac{\rho}{\rho_0} = 1$, $\dfrac{T}{T_0} = 1$, and Velocity is extrapolated from interior domain	All the variables are extrapolated from the interior domain

(a)   (b)

(c)   (d)
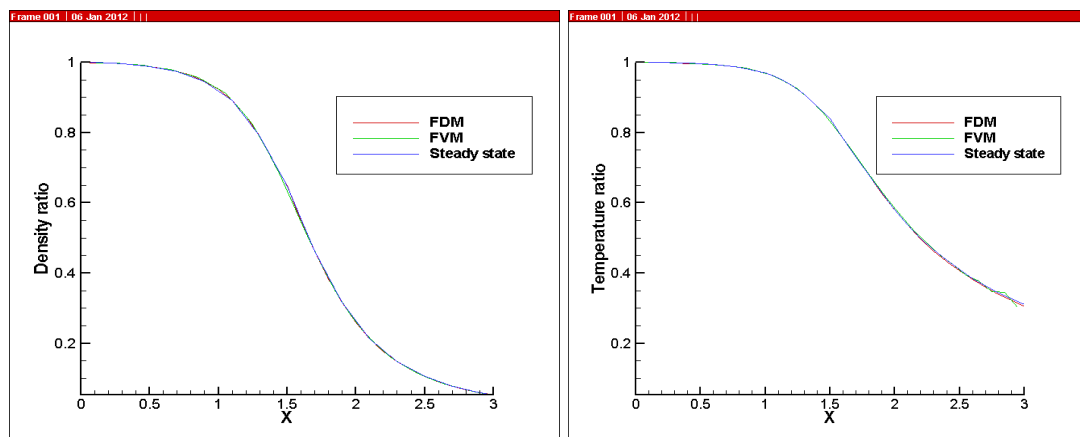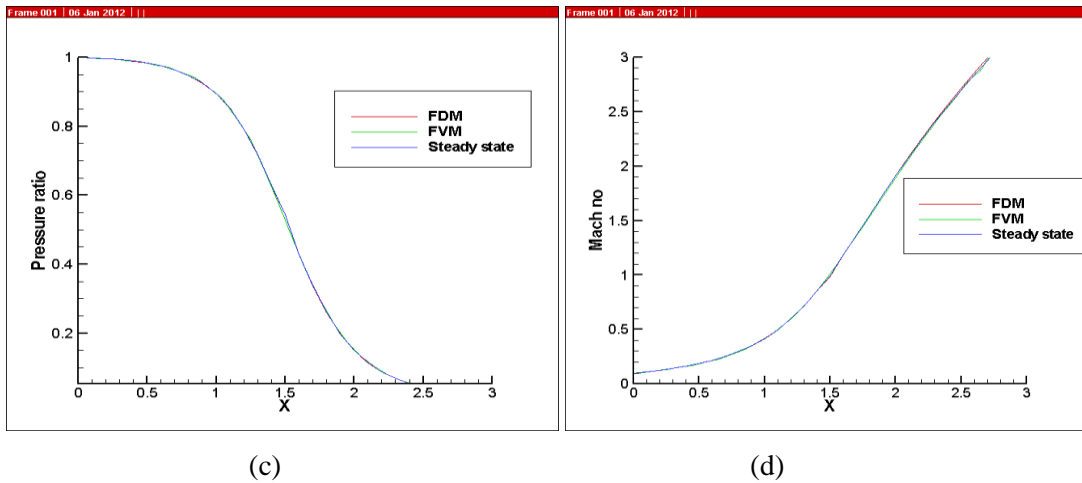
Figure 3.1 Results for subsonic to supersonic flow, where (a), (b) ,(c), and (d) shows density ratio, temperature ratio, pressure ratio ,and Mach number along the length of nozzle.

From Figure 3.1 it can be noticed that the results obtained by both FDM and FVM for density ratio, temperature ratio, pressure ratio and Mach no are in good agreement with the steady state results given by Anderson [2].

3.2.2   Subsonic-subsonic flow

Initial Conditions:-

Table 3.5 Initial conditions for subsonic to subsonic flow without shock

Distance	$0 \leq x \leq 3$
ρ	$1 - 0.023x^{'}$
T	$1 - 0.009333x^{'}$
v	$0.05 + 0.11x^{'}$

Boundary Conditions:-

Table 3.6 Boundary conditions for subsonic to subsonic flow without shock

Subsonic inlet	Subsonic outlet
$\frac{\rho}{\rho_0} = 1$, $\frac{T}{T_0} = 1$, and	$\frac{p}{p_0} = 0.93$
Velocity is extrapolated from interior domain	Other variables are extrapolated from the interior domain

33

(a)

(b)

(c)

(d)
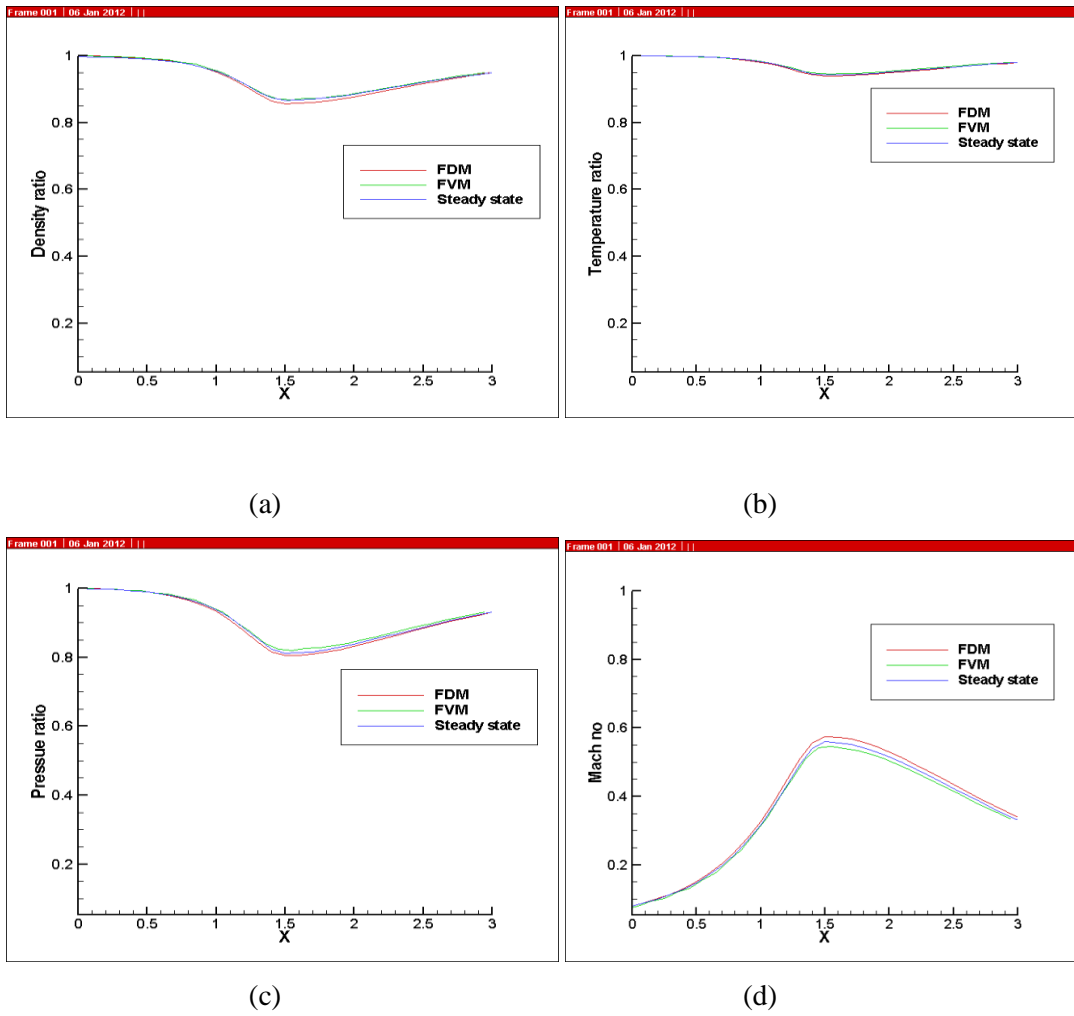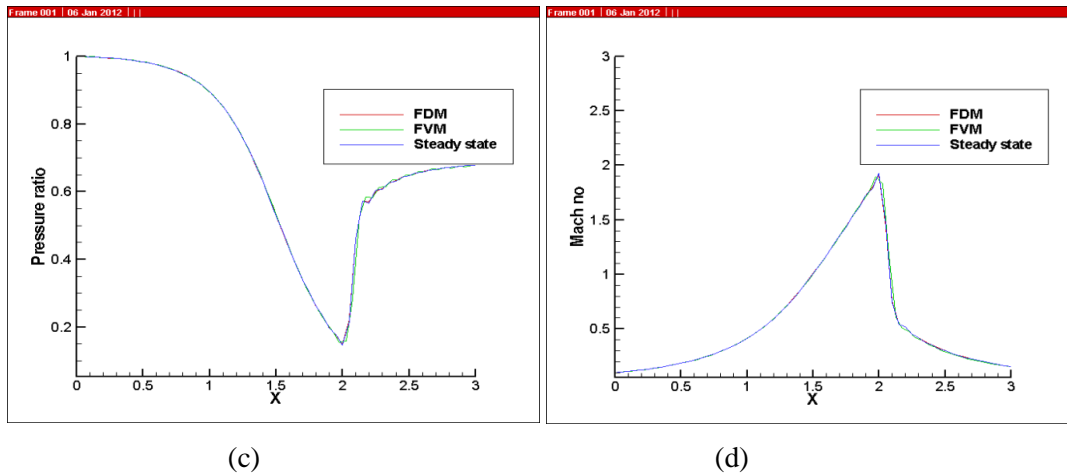
Figure 3.2 Results for subsonic to subsonic flow without shock through convergent nozzle, where (a), (b) ,(c), and (d) shows density ratio, temperature ratio, pressure ratio ,and Mach no along the length of nozzle.

From Figure 3.2 it can be seen that for subsonic inlet to subsonic outlet case density ratio, temperature ratio, pressure ratio, and Mach no by FDM and FVM method are in good agreement with the steady state results given in the Anderson [2].

Extrapolation of variables is done as follows;

$$(U_1)_{n+1} = 1.5(U_1)_n - 0.5(U_1)_{n-1}$$
$$(U_2)_{n+1} = 1.5(U_2)_n - 0.5(U_2)_{n-1}$$

3.2.3 Subsonic-subsonic flow with shock

Initial Conditions:-

Table 3.7 Initial conditions for subsonic to subsonic flow with shock

Distance	$0 \leq x \leq 0.5$	$0.5 \leq x \leq 1.5$	$1.5 \leq x \leq 2.1$	$2.1 \leq x \leq 3$
ρ	1	$1 - 0.366(x' - 0.5)$	$0.634 - 0.702(x' - 1.5)$	$0.5892 + 0.1022(x' - 2.1)$
T	1	$1 - 0.167(x' - 0.5)$	$0.833 - 0.4908(x' - 1.5)$	$0.93968 + 0.0622(x' - 2.1)$
ρv	0.59			

Boundary Conditions:-

Table 3.8 Boundary conditions for subsonic to subsonic with shock

Subsonic inlet	Subsonic outlet
$\dfrac{\rho}{\rho_0} = 1$, $\dfrac{T}{T_0} = 1$, and Velocity is extrapolated from interior domain	$\dfrac{p}{p_0} = 0.6784$ Other variables are extrapolated from the interior domain

(a)   (b)

35

(c)   (d)
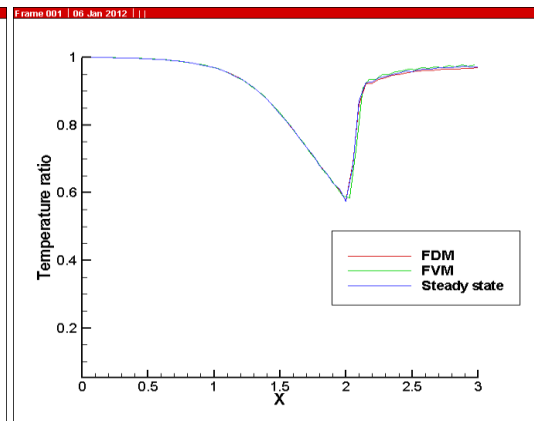
Figure 3.3 Results for subsonic to subsonic flow with shock through convergent divergent nozzle, where (a), (b) ,(c), and (d) shows density ratio, temperature ratio, pressure ratio ,and Mach number along the length of nozzle.

From figure 3.3 it can be seen that the shock wave is been captured by both FDM and FVM methods and density ratio, temperature ratio, pressure ratio, and Mach number are in good agreement with the results given by Anderson [2].

3.3   Shock tube problem

A simple one dimensional Sod shock tube problem [25] is solved to test the code for problems with the shock wave behavior.

The tube is filled with a gas as shown in the figure 3.4 at different states on the left and right side of a diaphragm. The gas states have different densities and pressures and are at rest. At time $t = 0$, the diaphragm is broken and if it is assumed that viscous effects are negligible and the tube is of infinite length (reflection waves are zero), then the unsteady Euler equations for a one-dimensional flow can be solved analytically with a family of characteristics travelling to the left and right of the diaphragm. If the left side contains the gas at the highest pressure, the right state will expand in the left side region through expansion waves, whereas a compression wave will travel in the right direction.

Diaphragm

$p1, \rho1, u1$ $p2, \rho2, u2$
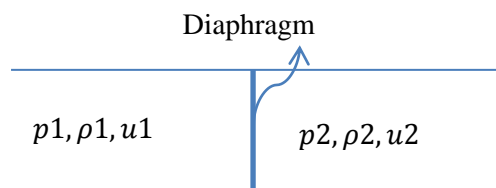
Figure 3.4. Shock tube.

36

Governing Equations:-

Continuity Equation

$$\frac{\partial \rho}{\partial t} + \frac{\partial \rho u}{\partial x} = 0 \tag{3.8}$$

Momentum Equation:-

$$\frac{\partial (\rho u)}{\partial t} + \frac{\partial (\rho u^2 + p)}{\partial x} = 0 \tag{3.9}$$

Energy Equation:-

$$\frac{\partial e}{\partial t} + \frac{\partial [u(e + p)]}{\partial x} = 0 \tag{3.10}$$

Where ρ is the density of the fluid, u is the fluid velocity, e is the energy per unit volume, and p is the pressure which is given by the equation of state.

$$p = (\gamma - 1)\left(e - \frac{1}{2}\rho u^2\right) \tag{3.11}$$

Initial conditions:-

Table 3.9 Initial conditions for shock tube

Distance	$x \leq \frac{1}{2}$	$x > \frac{1}{2}$
ρ	1	0.125
p	1	0.1
u	0	0

Here just transient behavior is studied so for boundary conditions at both the ends all the variables are just extrapolated

<p style="text-align:center">(a)   (b)</p>
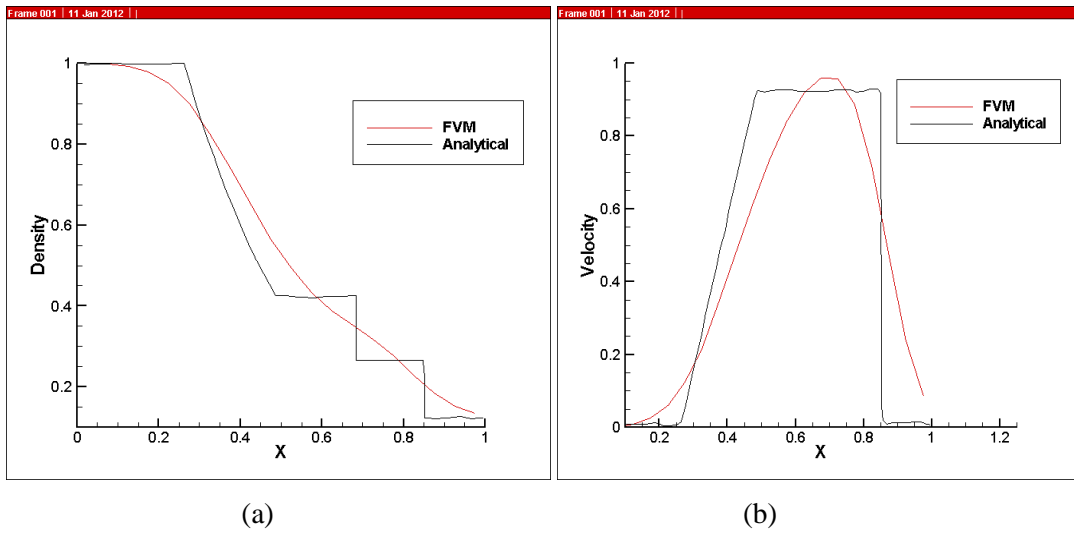
Figure 3.5 Results for shock tube problem , where (a) and (b) shows the density and velocity variation across the shock tube after 0.2 secs.

Chapter 4

Results and Discussion – 2D Problems

4.1 Pseudo 2D dimensional nozzle problem.

Test case problems discussed in the Quasi one dimensional nozzle flow chapter are now solved by the 2-D Euler equation. Here the same area equations of the nozzle been used to generate the grid of 30X10 cells. These 2D convergent divergent nozzles are then divided into 10 equivalent convergent divergent tubes. Here flow of fluid is allowed only in the longitudinal direction by limiting flow from top and bottom as shown in the Figure 4.1. So effectively this actual 2 dimensional problem boils down to several Quasi 1D problems being solved simultaneously. This (i.e. using the 2-D equations to obtain the Quasi 1-D result) is being done only as an internal check of the FVM implementation of the Euler equations.

The IC's and BC's are similar to Quasi one dimensional cases. All these cases are solved by actual MacCormack scheme.
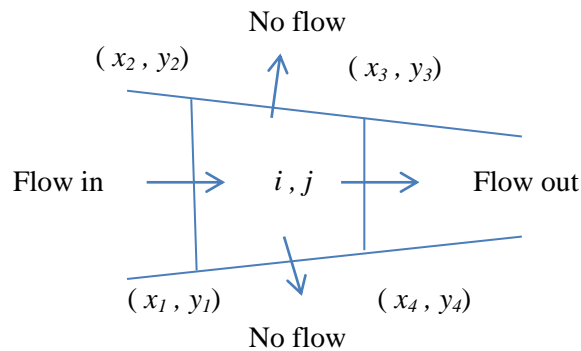
Figure 4.1 Flow constrained to flow through x-direction

Vertical component of velocity in the initial conditions is specified by making use of the horizontal component of velocity and average slope of cell. Average slope is given by,

$$Avg.slope = \frac{(y_2 + y_3) - (y_1 + y_4)}{2(x_2 - x_1)}$$

Vertical component of velocity is given by,

$$v = u\left(\frac{(y_2 + y_3) - (y_1 + y_4)}{2(x_2 - x_1)}\right)$$

Mesh used for convergent divergent and convergent nozzle is of 30 x 10 cells as shown below
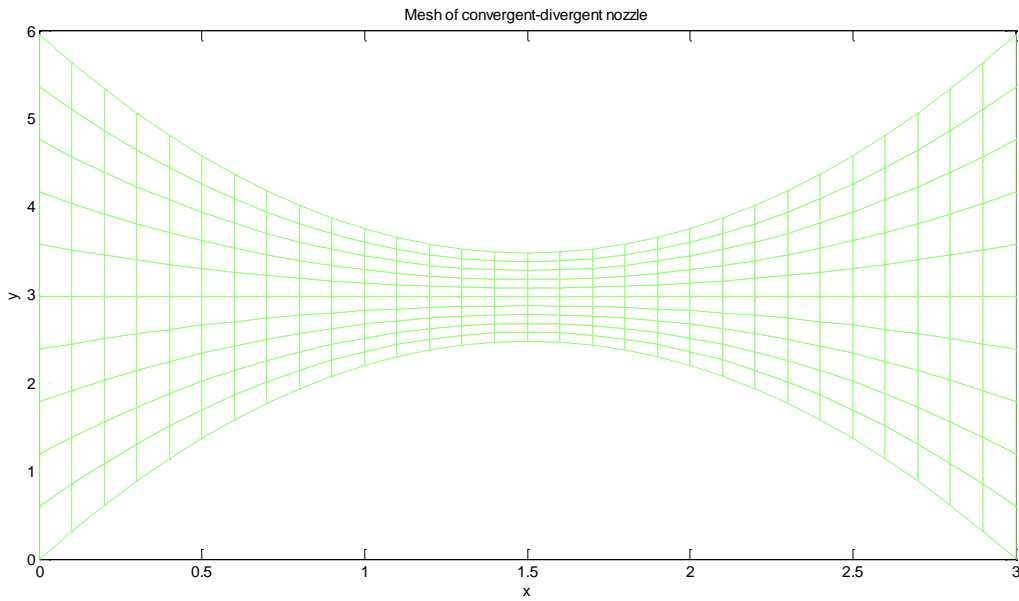
(a)
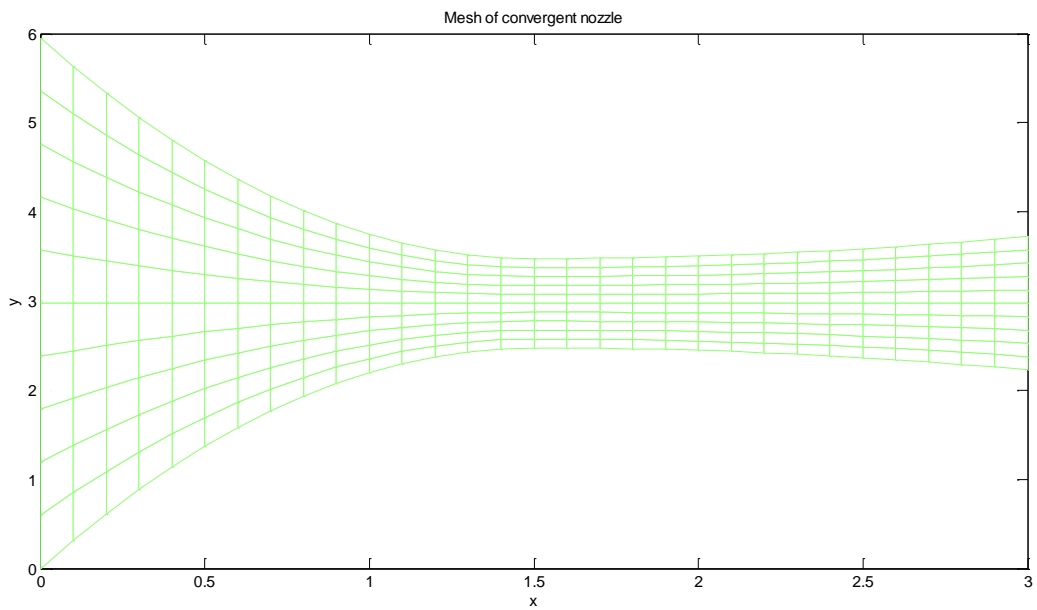
(b)

Figure 4.2 Mesh used for CD nozzle (a) and convergent nozzle (b)

As all these 10 tubes are equivalent, so density, temperature, pressure and Mach no. of all tubes at a particular section will be same. Results of these three test cases are as follows.

4.1.1 Subsonic-supersonic flow:-

Initial conditions:-

Distance	$0 \leq x \leq 0.5$	$0.5 \leq x \leq 1.5$	$1.5 \leq x \leq 3$
ρ'	1	$1 - 0.366(x' - 0.5)$	$0.634 - 0.3879(x' - 1.5)$
T'	1	$1 - 0.167(x' - 0.5)$	$0.833 - 0.3507(x' - 1.5)$
$\rho' u'$	0.59		
v'	u'_X Avg. slope of a cell		

Boundary conditions:-

Subsonic inlet	Supersonic outlet
$\rho' = 1, T' = 1$, and $\rho' u'$ and $\rho' v'$ are extrapolated from interior domain	All the variables are extrapolated from the interior domain

Density plot for psuedo Subsonic to Supersonic flow

(a)

Pressure plot for psuedo Subsonic to Supersonic flow

(b)

Mach no plot for psuedo Subonic to Supersonic flow
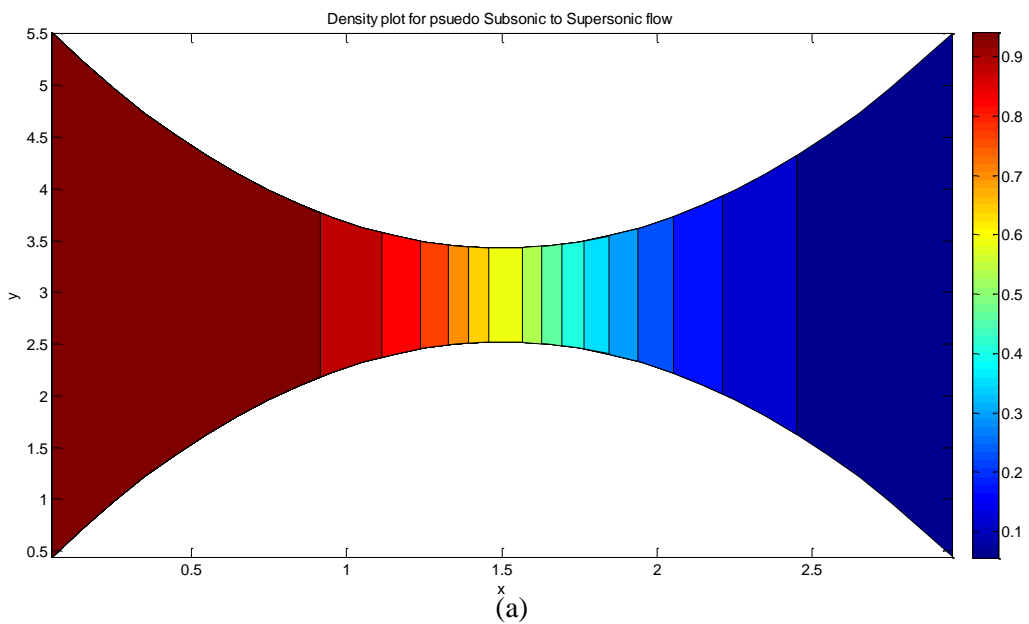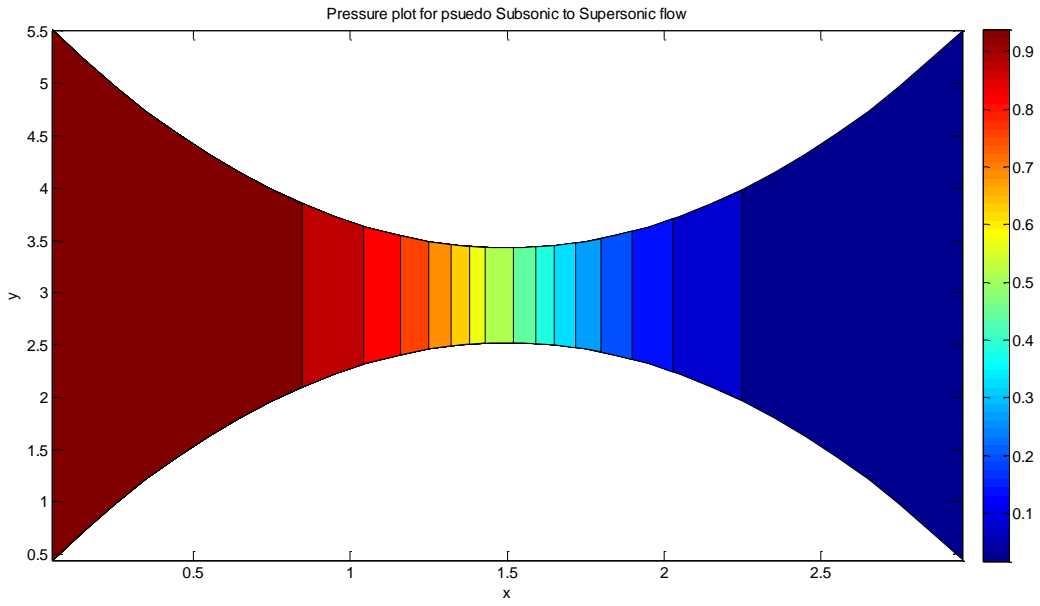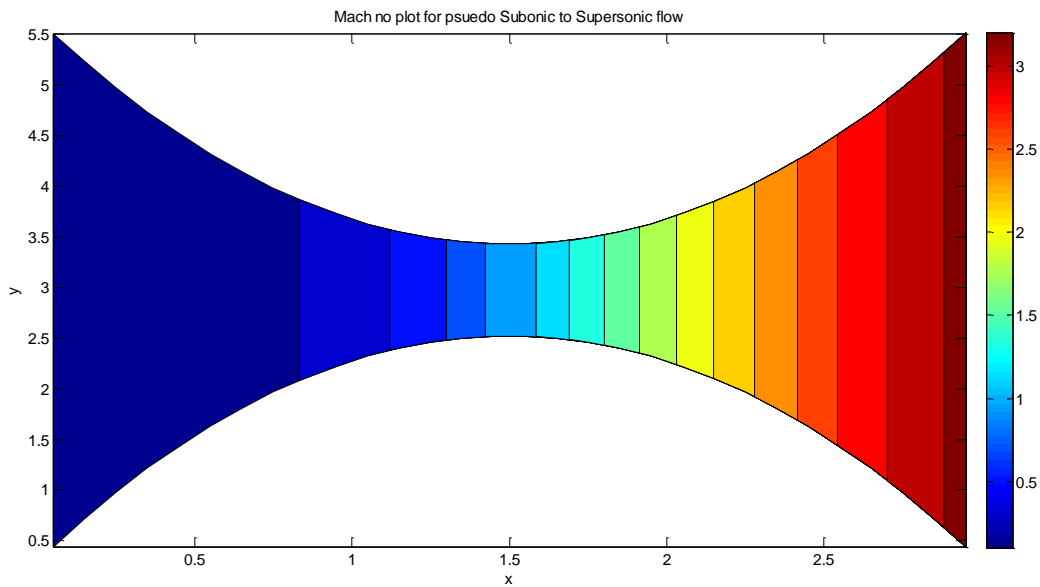
(c)

Figure 4.3 Contour plots of density (a), pressure (b), and Mach number (c) for Subsonic to Supersonic flow.

This can be noted from Fig.4.3 that density, pressure and Mach no of each tube is same. Density and Mach no of each tube is compared with the Quasi 1D flow results as follows.

(a)	(b)
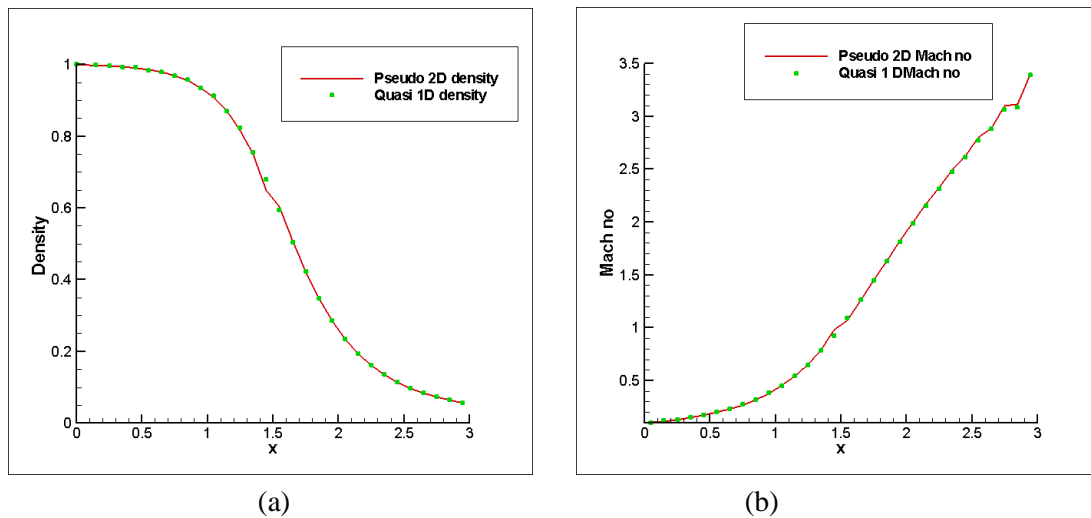
Figure 4.4 Density (a), and Mach number (b) comparison for pseudo 2D Subsonic to Supersonic flow.

From Fig. 4.4 it can be noted that the pseudo 2D results are in good agreement with Quasi 1D results.
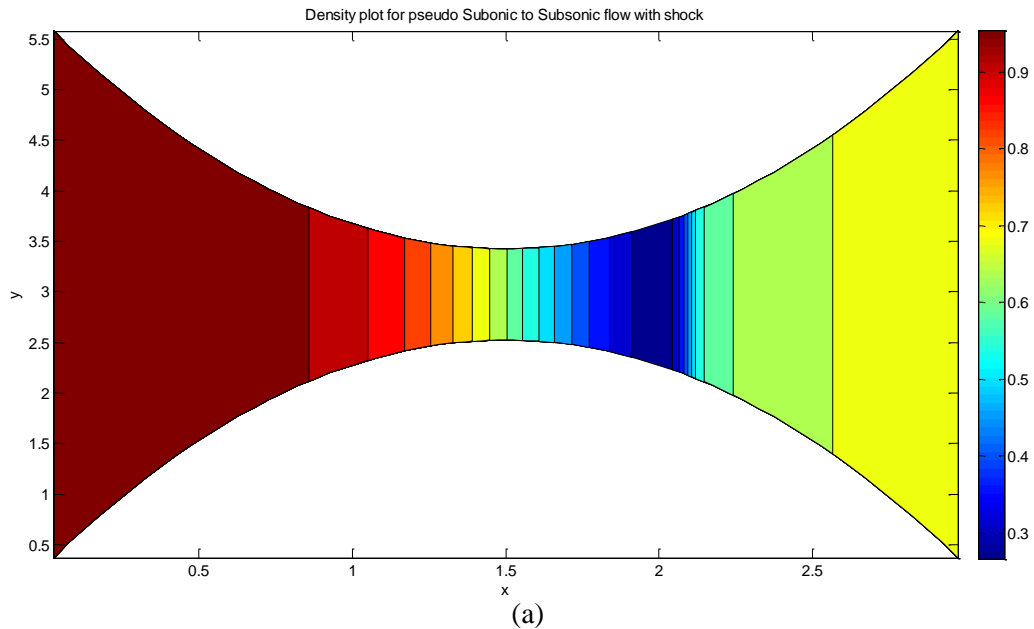
4.1.2   Subsonic-subsonic flow:

Initial conditions:-

Distance	$0 \leq x \leq 3$
$\rho^{'}$	$1 - 0.023x^{'}$
$T^{'}$	$1 - 0.009333x^{'}$
$u^{'}$	$0.05 + 0.11x^{'}$
$v^{'}$	$u^{'}_{X}$Avg. slope of cell

Boundary Conditions:-

Subsonic inlet	Subsonic outlet
$\rho^{'} = 1, T^{'} = 1$, and $\rho^{'}u^{'}$ and $\rho^{'}v^{'}$ are extrapolated from interior domain	$\dfrac{p}{p_0} = 0.93$ Other variables are extrapolated from the interior domain

Results of subsonic to subsonic flow (without shock) through convergent nozzle results are as follows.

(a)
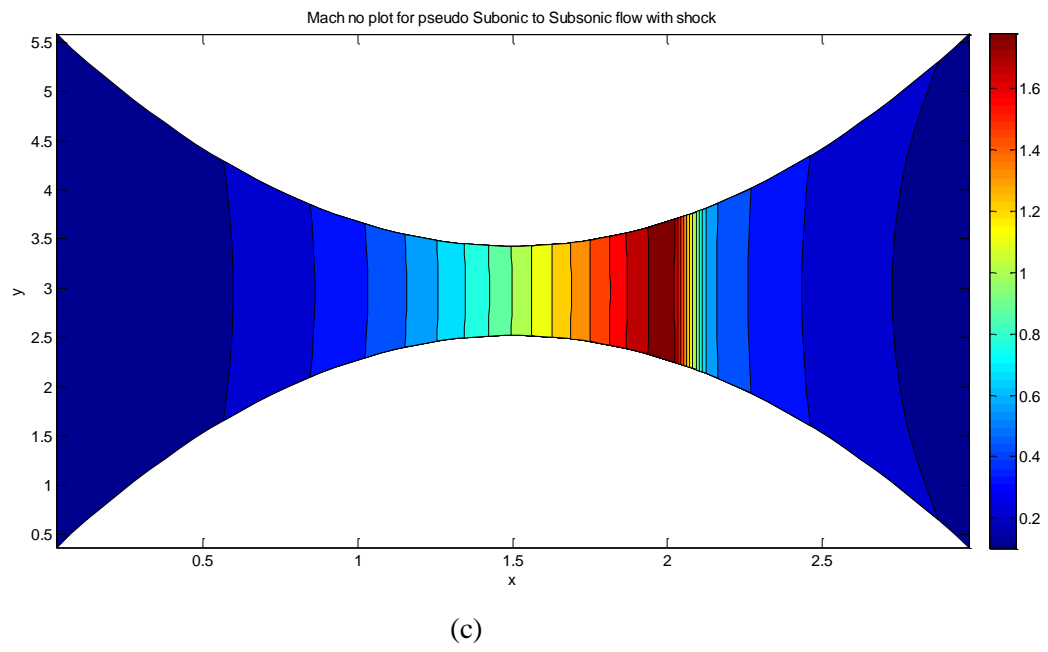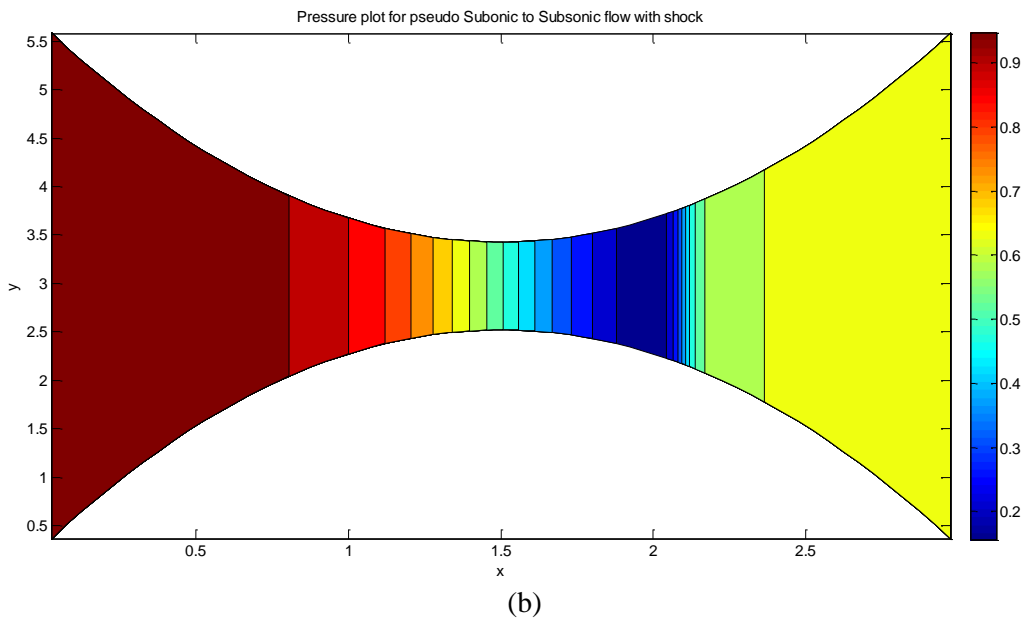

(b)

Mach no plot for pseudo Subonic to Subsonic flow without shock
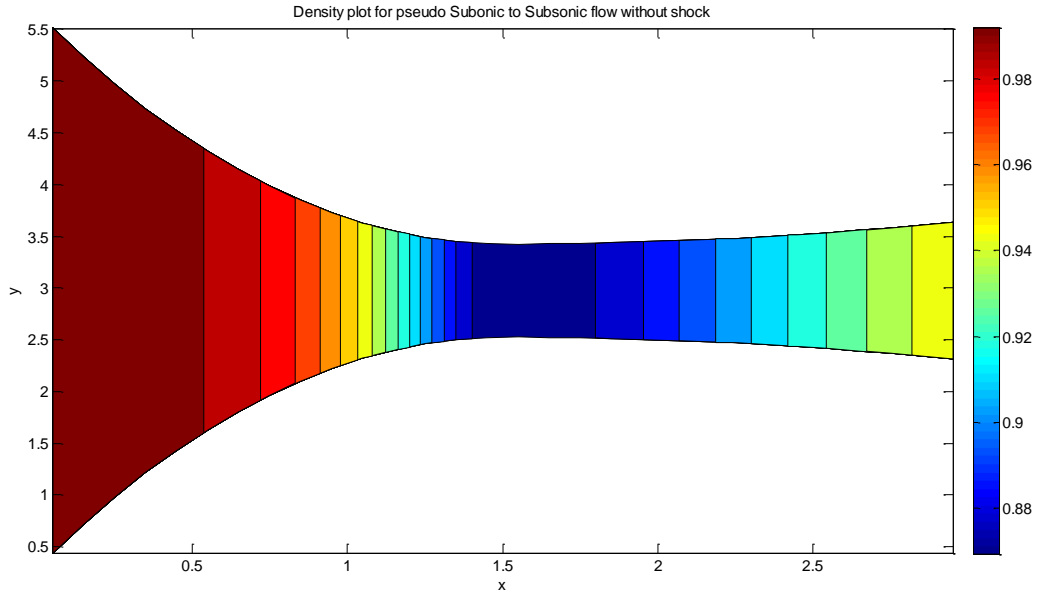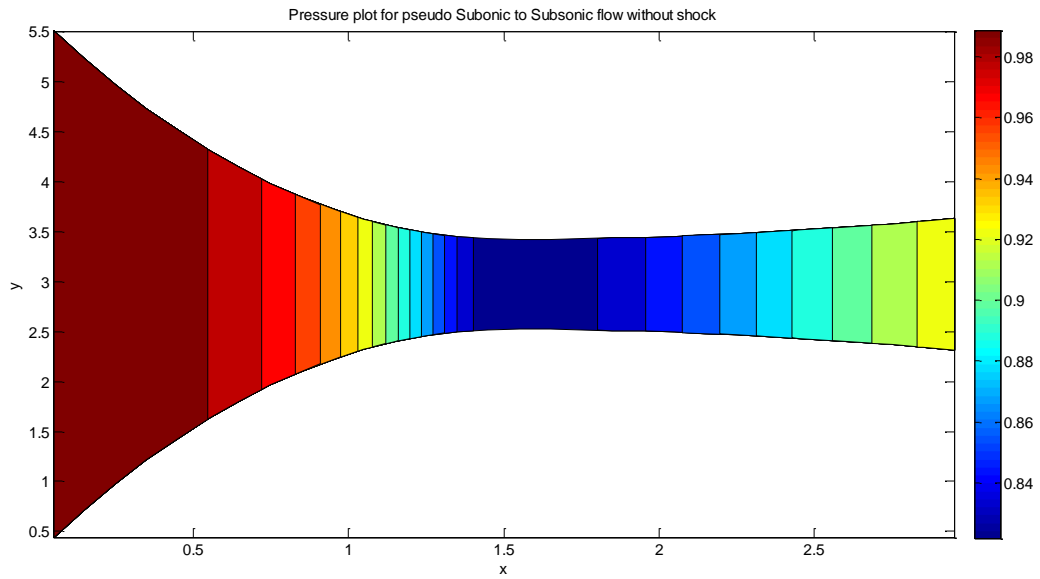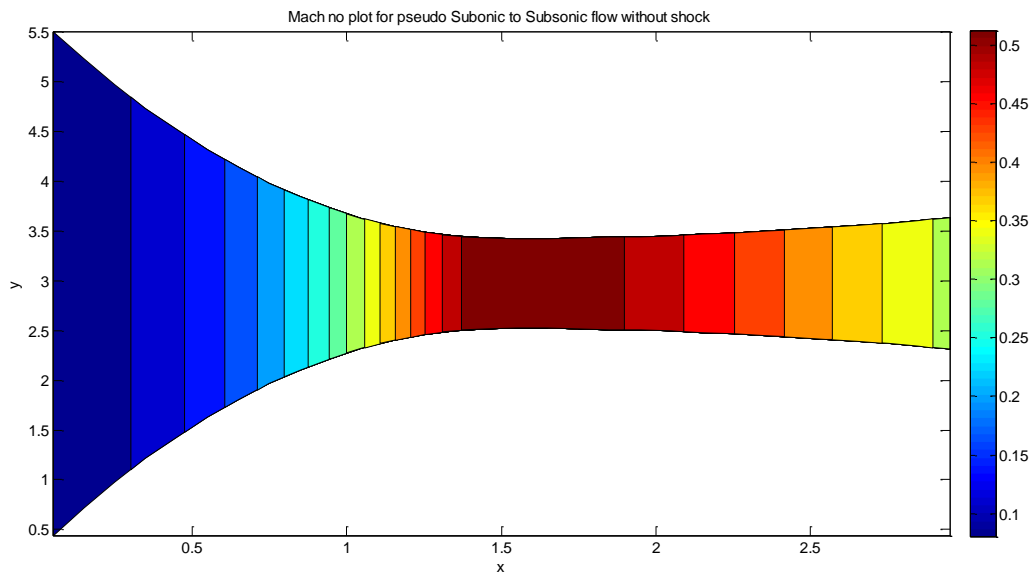
(c)

Figure 4.5 Contour plots of density (a), pressure (b), and Mach number (c) for Subsonic to subsonic flow

2D density and Mach no are compared with the Quasi 1D density and Mach no as follows,
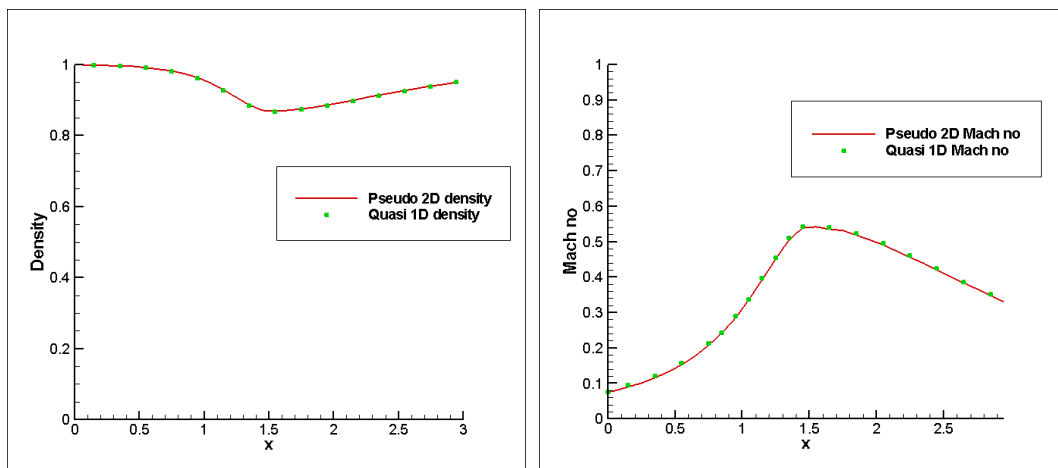
(a)   (b)

Figure 4.6 Density (a), and Mach number (b) comparison for pseudo 2D Subsonic to subsonic flow with Quasi 1D flow.

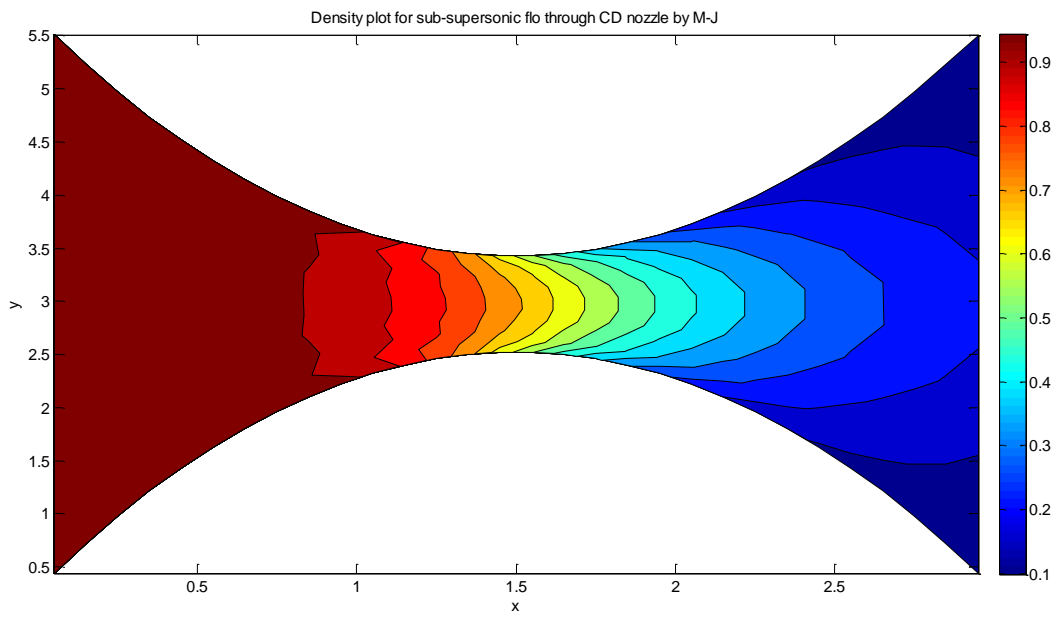From Fig. 4.6 it can be noted that the pseudo 2D results are in good agreement with Quasi 1D results.

45

4.1.3 Subsonic-subsonic flow with shock:-

Initial conditions:-

Distance	$0 \le x \le 0.5$	$0.5 \le x \le 1.5$	$1.5 \le x \le 2.1$	$2.1 \le x \le 3$
ρ'	1	$1-0.366(x'-0.5)$	$0.634-0.702(x'-1.5)$	$0.5892+0.1022(x'-2.1)$
T'	1	$1-0.167(x'-0.5)$	$0.833-0.4908(x'-1.5)$	$0.93968+0.0622(x'-2.1)$
$\rho'u'$	0.59			
v'	u'_X Avg. slope of cell			

Boundary conditions:-

Subsonic inlet	Subsonic outlet
$\rho'=1, T'=1$, and $\rho'u'$ and $\rho'v'$ are extrapolated from interior domain	$\dfrac{p}{p_0}=0.6784$ Other variables are extrapolated from the interior domain

Results of subsonic to subsonic flow with shock through convergent divergent nozzle are as follows

(a)

Pressure plot for pseudo Subonic to Subsonic flow with shock

(b)

Mach no plot for pseudo Subonic to Subsonic flow with shock

(c)

Figure 4.7 Contour plots of density (a), pressure (b), and Mach number (c) for Subsonic to Subsonic flow with shock.

Pseudo 2D density and Mach no are compared with the Quasi 1D density and Mach no as follows,
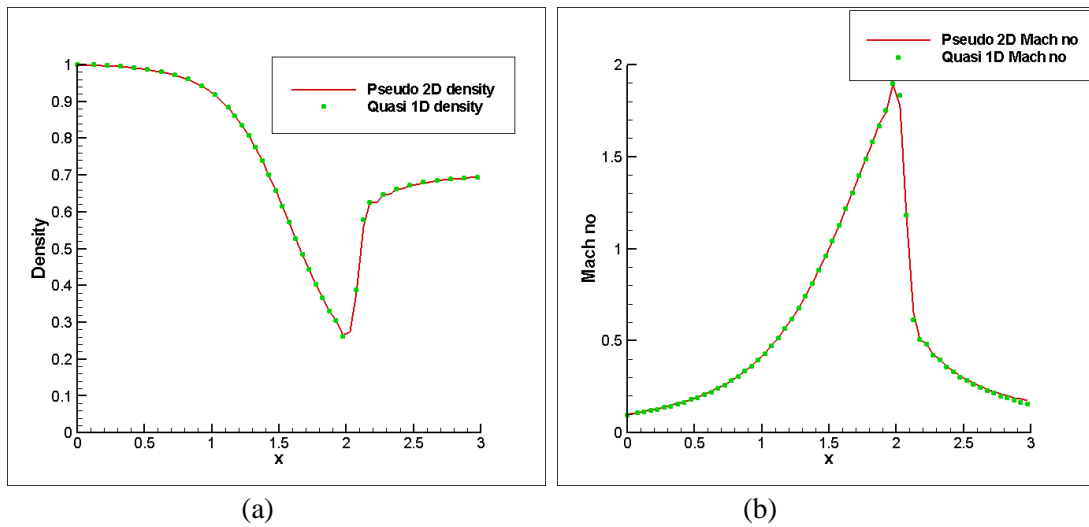
Figure 4.8 Density (a) and Mach number (b) comparison for pseudo 2D Subsonic to subsonic flow with shock with Quasi 1D flow.

From Fig. 4.8 it can be noticed that the pseudo 2D results are in good agreement with Quasi 1D results.

4.2   Two Dimensional nozzle flow problems.

Two of the previous test cases are now solved as fully 2-D problems(by removing the no-flux restriction between the vertically adjoint grid cells). The first one is subsonic to supersonic flow through convergent divergent nozzle; the second one is the subsonic to subsonic flow through the convergent nozzle. As mentioned in the previous pseudo two dimensional test cases in these test case flow through top and bottom faces except at the boundaries is not restricted .So this converts the 10 identical tube problem to actual 2 D problem. The third case subsonic to subsonic flow with shock didn't converge. Here for all these cases variant MacCormack scheme didn't work. It was found that the solutions to the 2-D problems could not be obtained without using some form of artificial viscosity.

The mesh, initial and boundary conditions used to solve these problems are identical to that used mentioned in the pseudo 2D test cases.

4.2.1   Subsonic-Supersonic flow through convergent-divergent nozzle.

This case is solved by MacCormack scheme with Jameson's artificial viscosity method. Results for this flow are as follows.

Density plot for sub-supersonic flo through CD nozzle by M-J

(a)

Temperature plot for sub-supersonic flow through CD nozzle by M-J
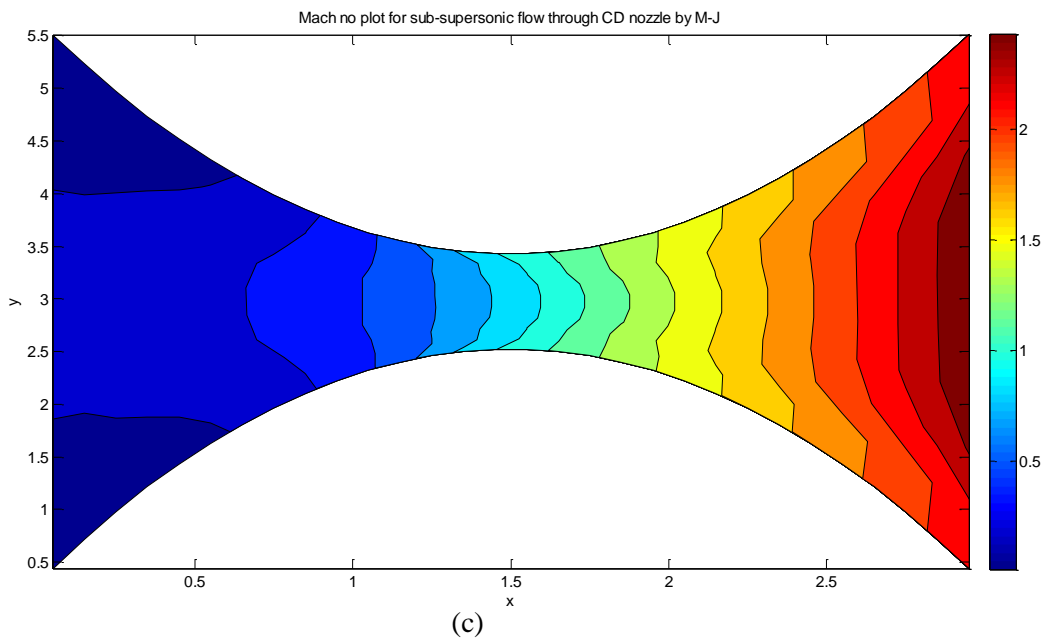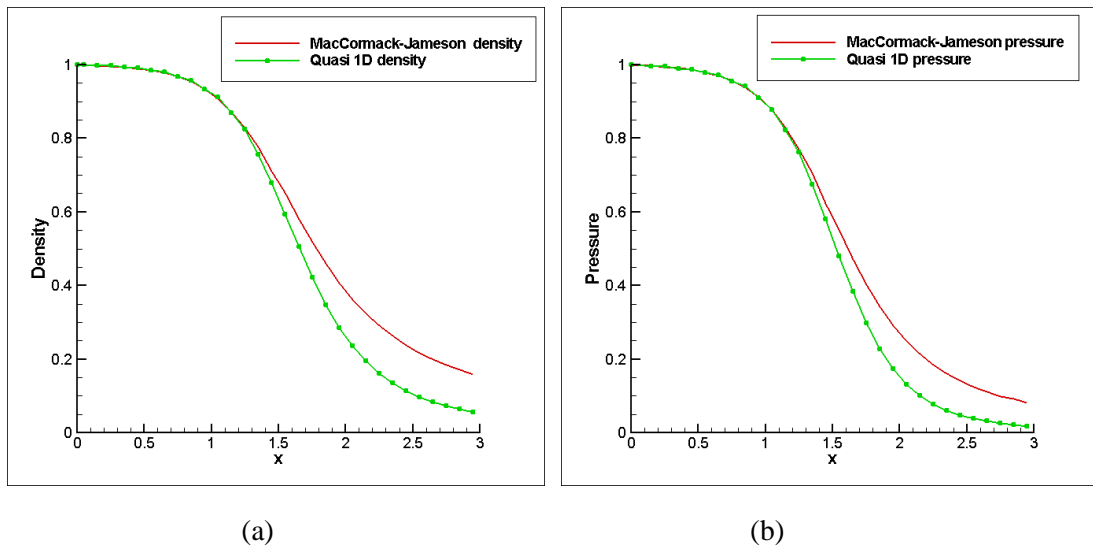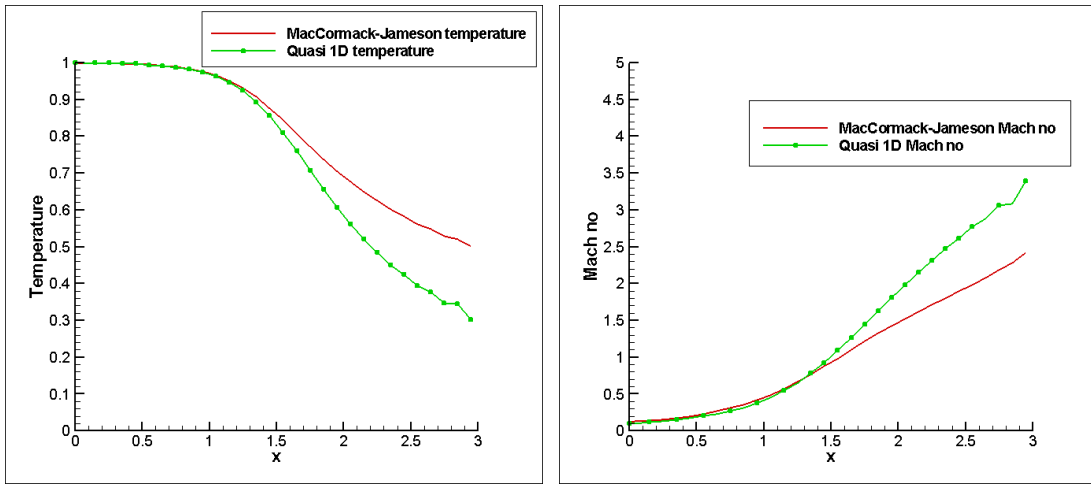
(b)

(c)
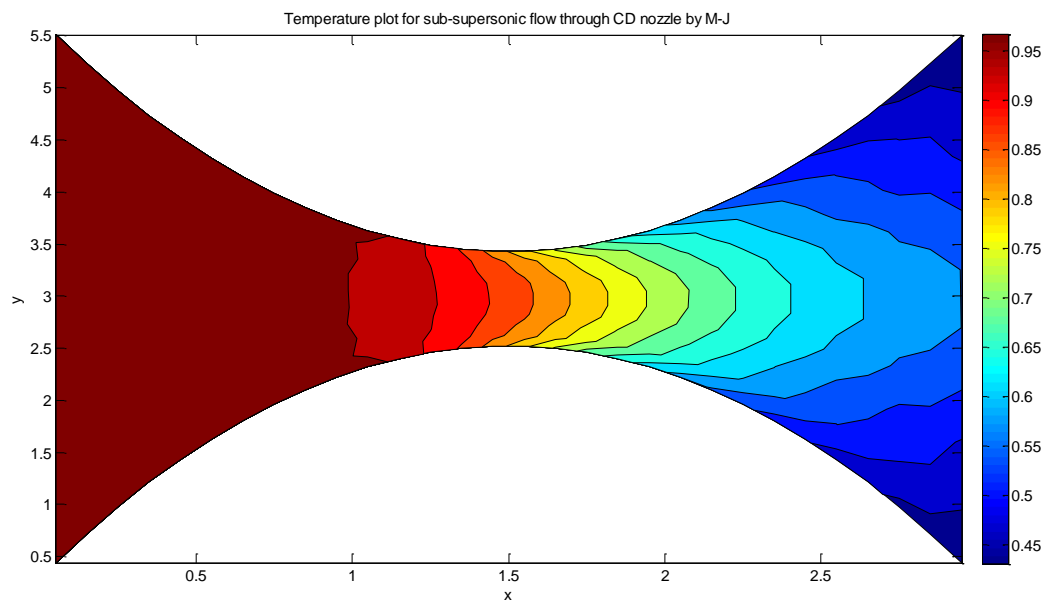
Figure 4.9 Contour plots of density (a), temperature (b), and Mach number (c) for Subsonic to Supersonic flow.

Comparison of average of density, pressure, temperature and Mach no. along vertical section are compared with the Quasi 1D flow results as follows


(a)   (b)

<center>(c)</center> <center>(d)</center>

<center>Figure 4.9 Comparison of density (a), pressure (b), temperature (c), and Mach number (d)</center>

<center>for Subsonic to Supersonic flow with Quasi 1D flow.</center>

It can be observed from Fig. 4.9 that quite significant differences exist between the Quasi 1-D (pseudo 2-D) and the full 2-D solutions, at least for supersonic flows.

4.2.2 Subsonic-Subsonic flow through convergent nozzle

This case of convergent nozzle with subsonic inlet and subsonic outlet without shock has been solved by two methods first with MacCormack scheme with Jameson's artificial viscosity and second with TVD-MacCormack scheme.

Results of this case by MacCormack scheme with Jameson's artificial viscosity are as shown below.

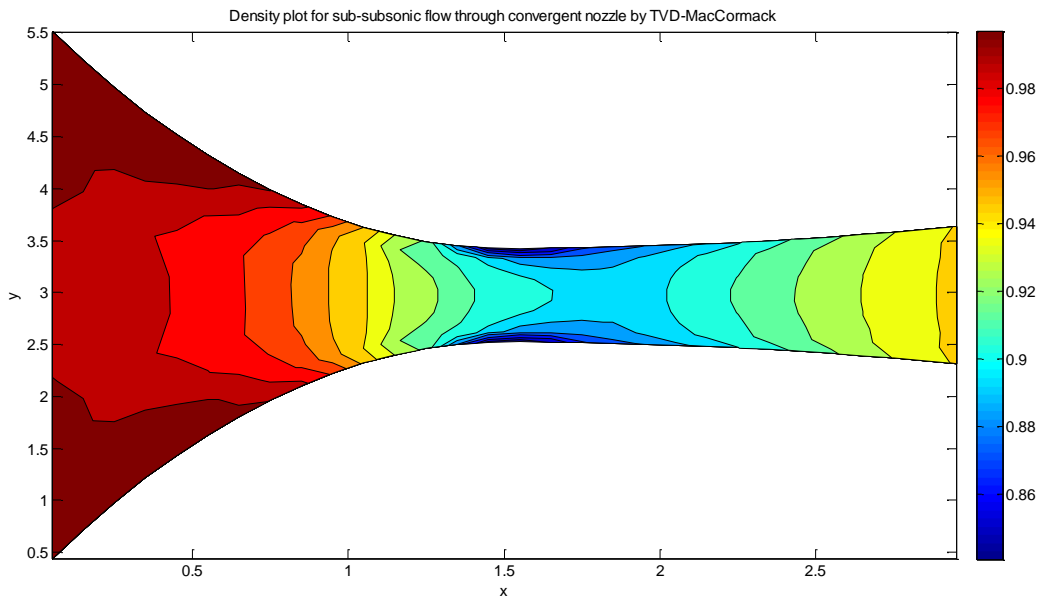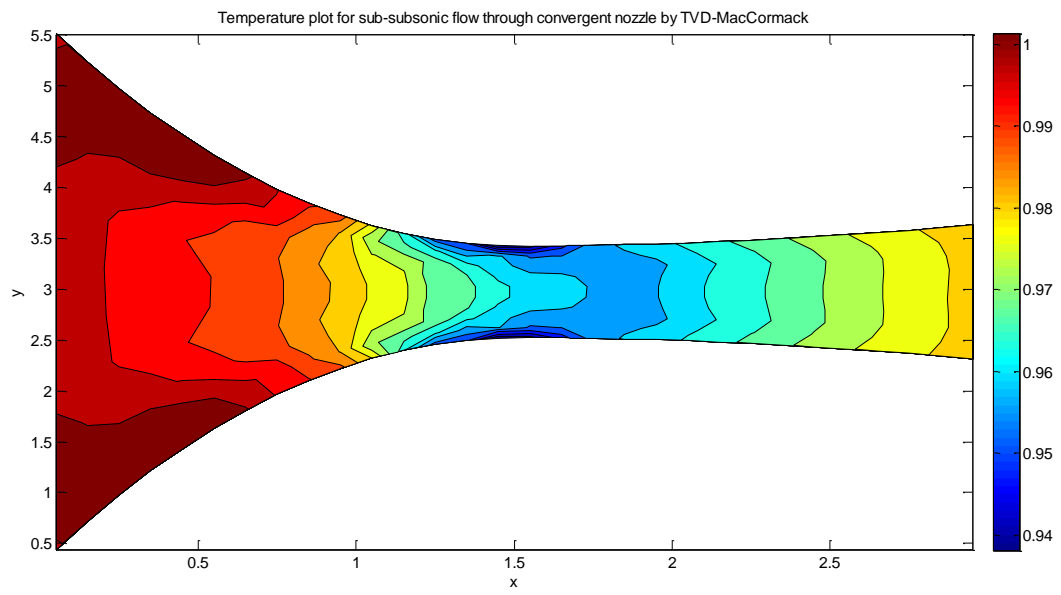<center>(a)</center>

(b)

(c)
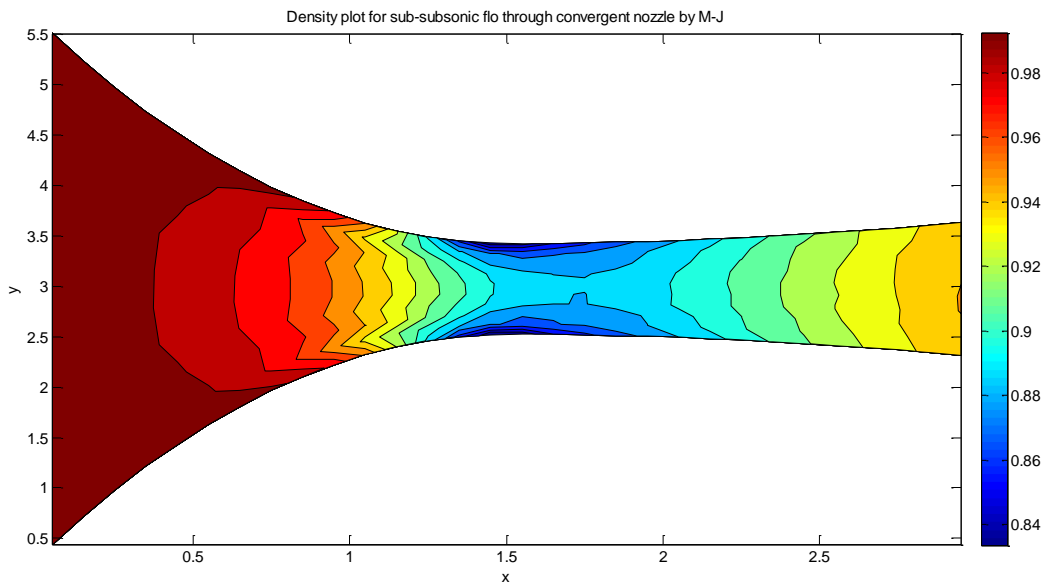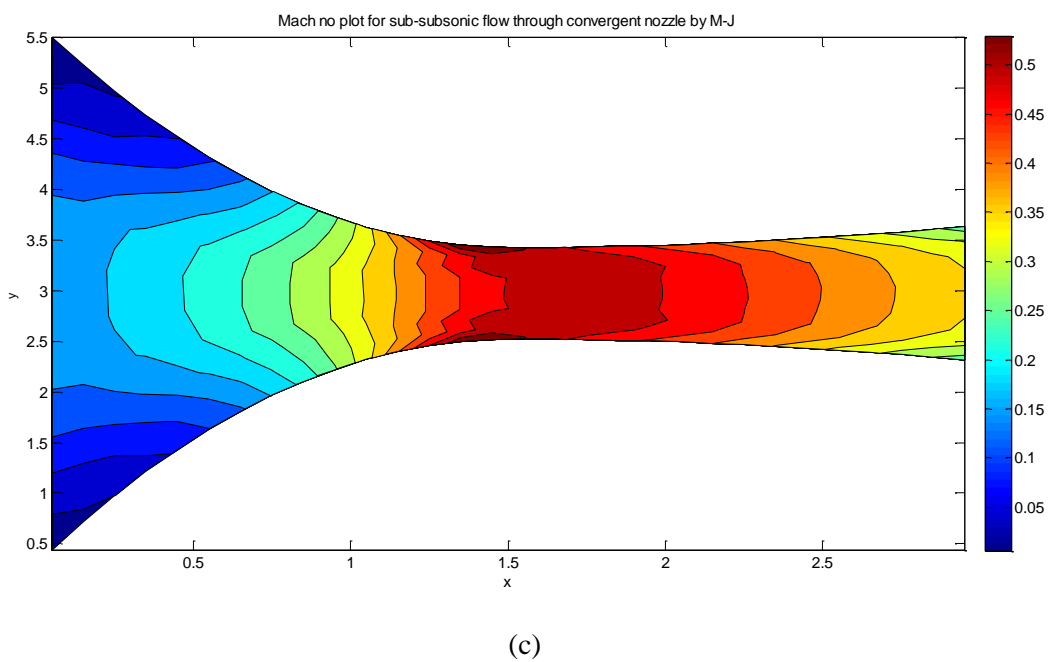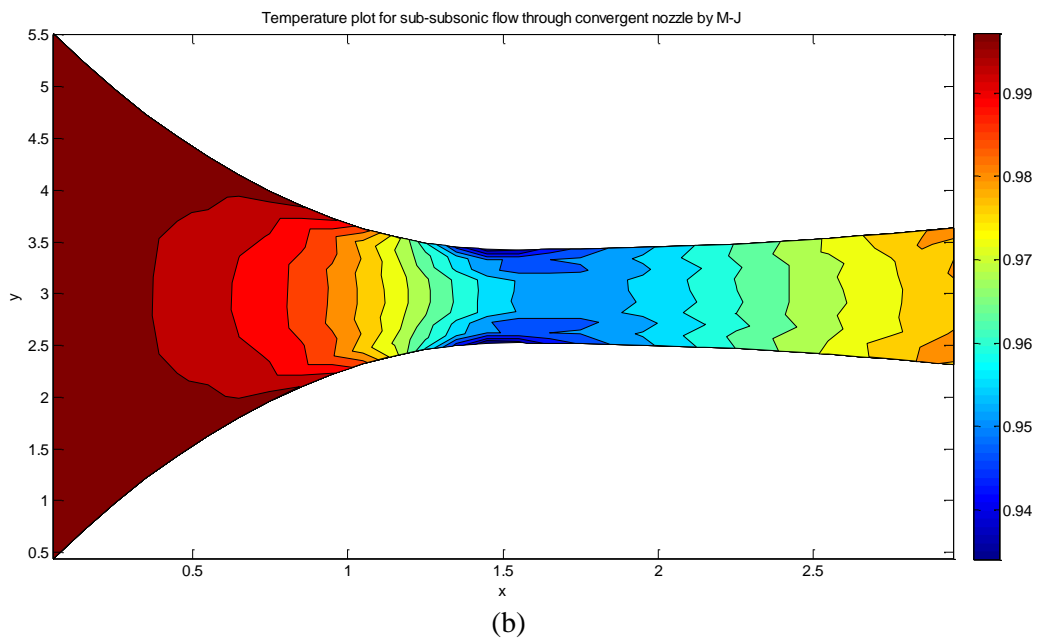
Figure 4.10 Contour plots of density (a), temperature (b), and Mach number (c) for Subsonic to Subsonic flow with MacCormack with Jameson's artificial viscosity.
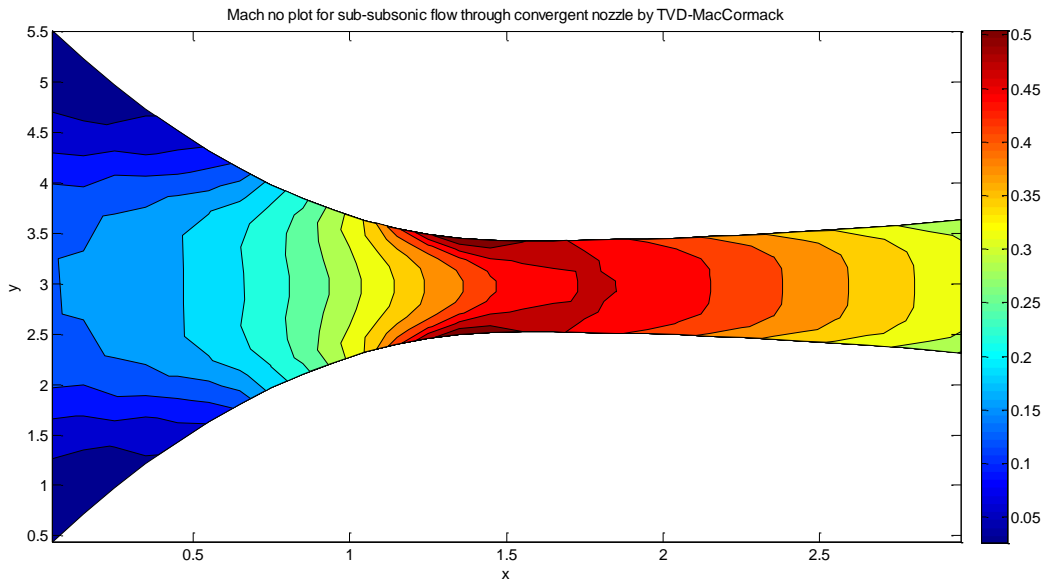
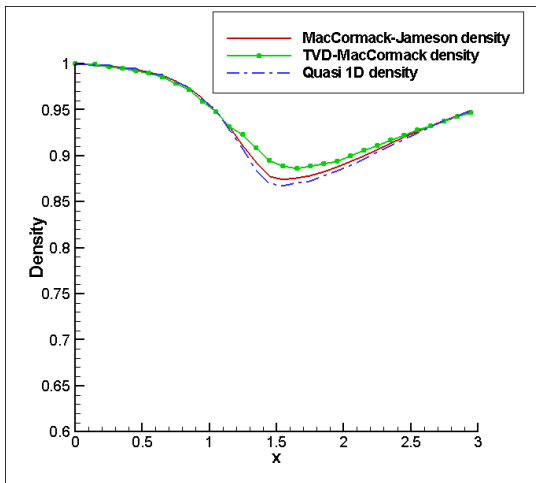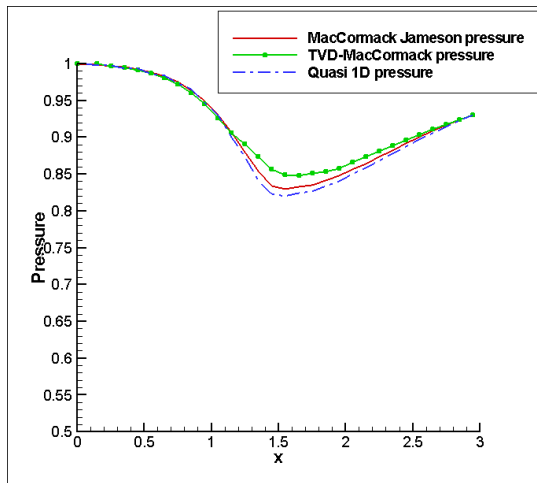Results of this case by TVD-MacCormack case are as shown below,

(a)

(b)

Figure 4.11 Contour plots of density (a), temperature (b), and Mach number (c) for Subsonic to Subsonic flow with TVD-MacCormack scheme.

(a)

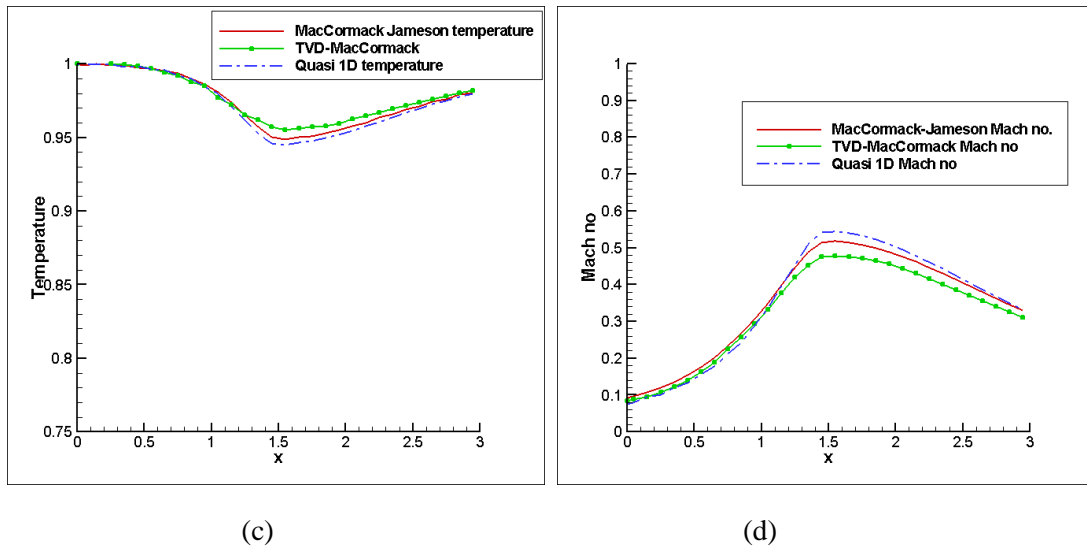(b)

54

(c)   (d)

Figure 4.12 shows the cross-sectional average values of the (a) density, (b) pressure, (c) temperature, and (d) Mach number obtained from the 2-D solutions being compared with the Quasi 1D flow results.

From Fig.4.12 it can be noticed that the results of both the schemes are in reasonably close agreement with the Quasi 1D flow results.

4.3   External flow over NACA 0012 airfoil at zero angle of attack.

Different test cases of flow over NACA 0012 airfoil have been done. For all these test cases airfoil geometry is generated by following equation.

$$y = \pm 0.6\left(0.2969\sqrt{x} - 0.1260x - 0.3516x^2 + 0.2843x^3 - 0.1036x^4\right)$$

As the airfoil is symmetric and the angle of attack is zero, only the upper half portion of the airfoil is used for all these test cases. Fig.4.13 shows flow domain and boundary conditions for NACA 0012 airfoil. Here height of the flow domain is taken as 10 times the chord length. Inlet boundary from airfoil leading edge is 10 times the chord length of airfoil; similarly the outlet is 10 times the chord length away from trailing edge.
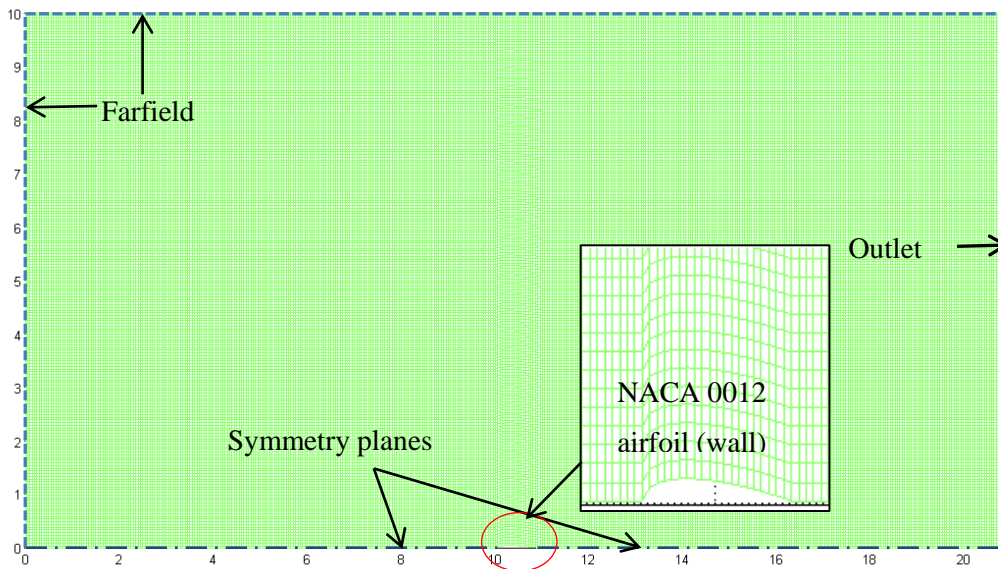
55

Figure 4.13 Flow domain and boundary conditions for NACA 0012 airfoil

Mesh:-

Two types of mesh have been used to solve these different test cases

1. With $\Delta x, \Delta y = 0.05$

2. With variation mesh size from minimum Δx of 0.01 over airfoil, for one unit chord length from leading edge and one unit chord length from trailing edge. From this mesh onwards towards farfield and towards outlet, mesh is varied from Δx of 0.02 to 0.05. Δy is 0.02 for whole domain.

For all test cases flow field is initialized with the isentropic properties corresponding to inlet Mach number. For external flows the flow will be going out from outlet to the free stream conditions, so all the variables at the outlet are extrapolated.

4.3.1   Inlet Mach number 0.5 with angle of attack (AOA) 0^0 :-

For this problem, the first mesh is used. Flow field is initialized with the isentropic properties corresponding to inlet Mach no. Velocity component from x-direction can be calculated from the inlet Mach number and isentropic temperature ratio.

Initial conditions:-

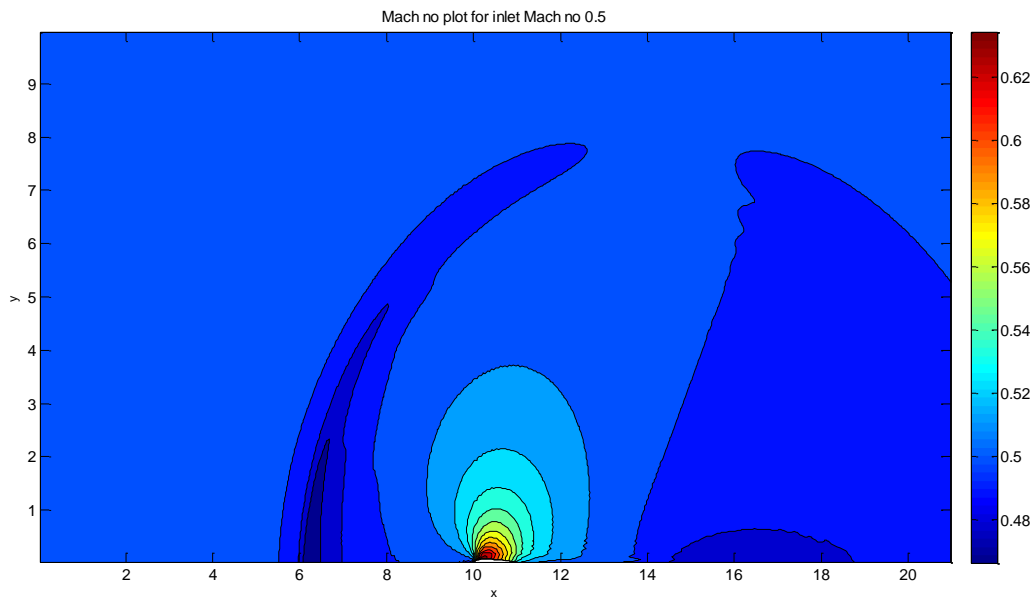Table 4.1 Initial conditions for Mach no. 0.5(AOA 0^0) flow over NACA 0012

$\rho^{'}$	0.8852
$p^{'}$	0.8430
$T^{'}$	0.9524
$u^{'}$	0.4880
$v^{'}$	0

Boundary conditions:-

Table 4.2 Boundary conditions for Mach no. 0.5(AOA 0^0) flow over NACA 0012

	Farfield boundary	Outlet
$\rho^{'}$	0.8852	All conservative variables are extrapolated from interior domain
$\rho^{'}u^{'}$	0.8852*0.4880	
$\rho^{'}v^{'}$	Extrapolated from interior domain	
$T^{'}$	0.9524	

Results of inlet Mach no. 0.5 (AOA 0^0) are as follows,

(a)
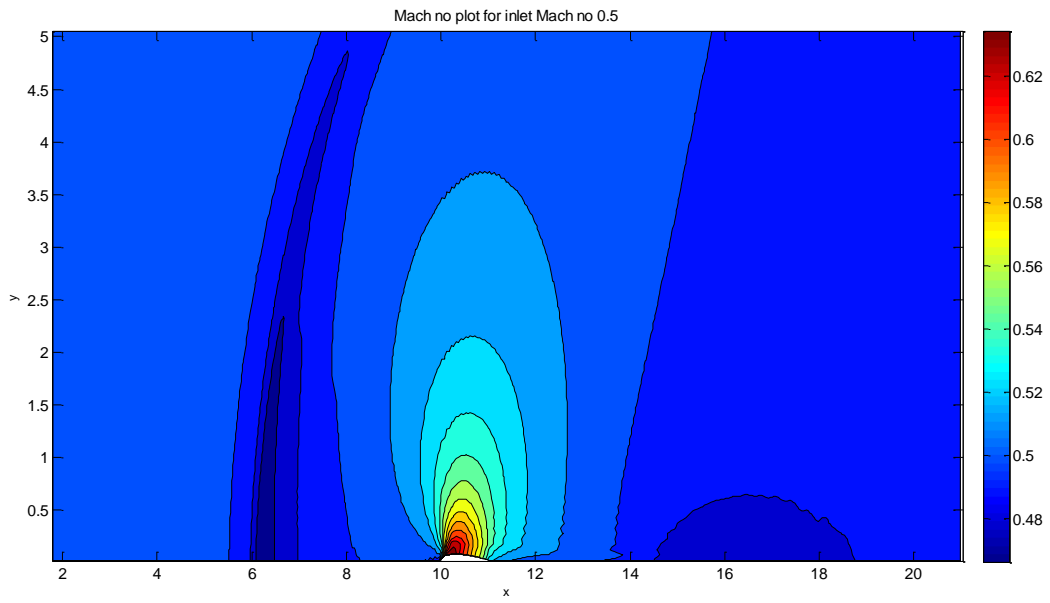
(b)

Figure 4.14 Contour plots of Mach no. over NACA 0012 airfoil for inlet Mach no. 0.5 (AOA 0^0), (a) full domain plot and (b) zoomed view.
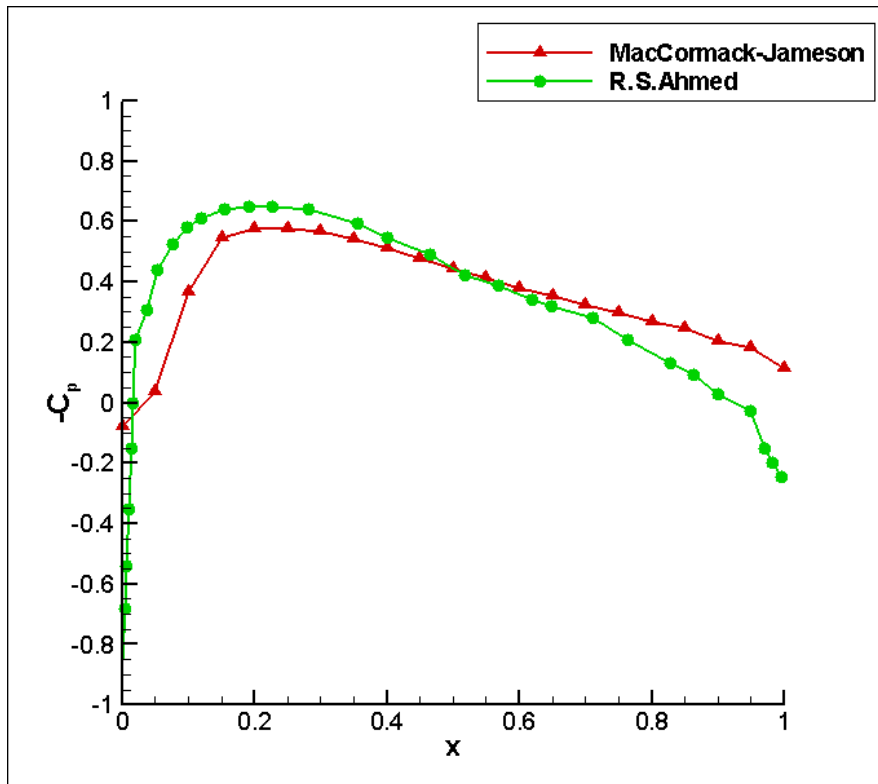

Figure 4.15 C_p distributions over NACA 0012 airfoil for inlet Mach no. 0.5(AOA 0^0)

The coefficient of pressure has been plotted in Fig.(4.15) along the chord length of the airfoil. From Fig.4.15 it can be noticed that the present results are in close agreement with the results given by R.S. Ahmed [20].

4.3.2   Inlet Mach number 0.8 with angle of attack (AOA) 0^0 :-

For this test case the second mesh is used.

Initial conditions:-

Table 4.3 Boundary conditions for Mach number. 0.8(AOA 0^0) flow over NACA 0012

$\rho^{'}$	0.7400
$p^{'}$	0.6560
$T^{'}$	0.8865
$u^{'}$	0.7532
$v^{'}$	0

Boundary conditions:-

Table 4.4 Boundary conditions for Mach number. 0.8(AOA 0^0) flow over NACA 0012

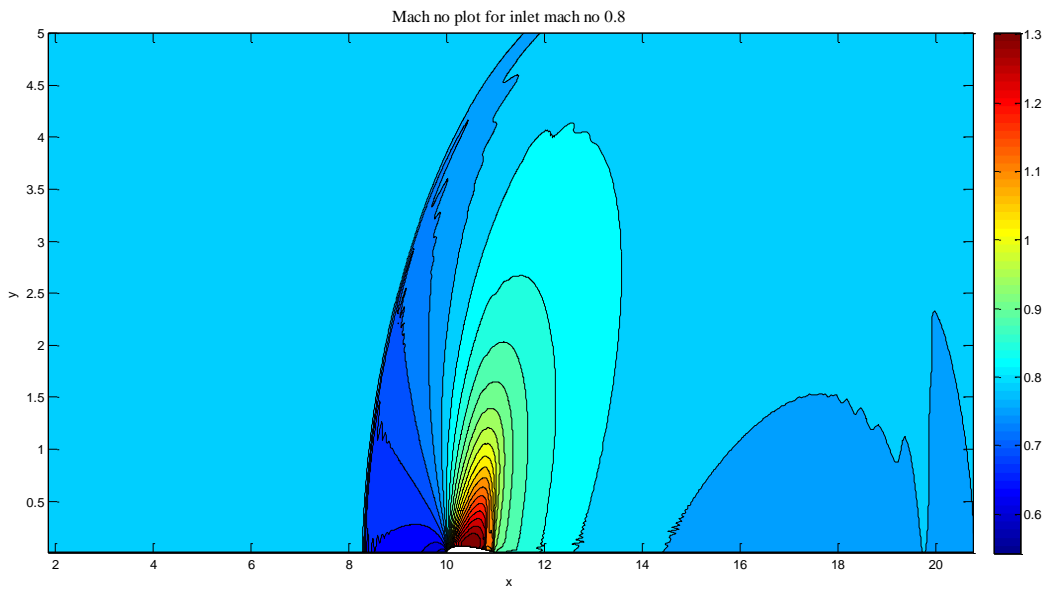|	Farfield boundary	Outlet
$\rho^{'}$	0.7400	All conservative variables are extrapolated from interior domain
$\rho^{'}u^{'}$	0.7400*0.7532	
$\rho^{'}v^{'}$	0	
$T^{'}$	0.8865	

Results of inlet Mach number 0.8 are as follows,

Figure 4.16 Contour plot of Mach number.0.8 over NACA 0012 airfoil for inlet Mach no. 0.8 (AOA 0^0), zoomed view
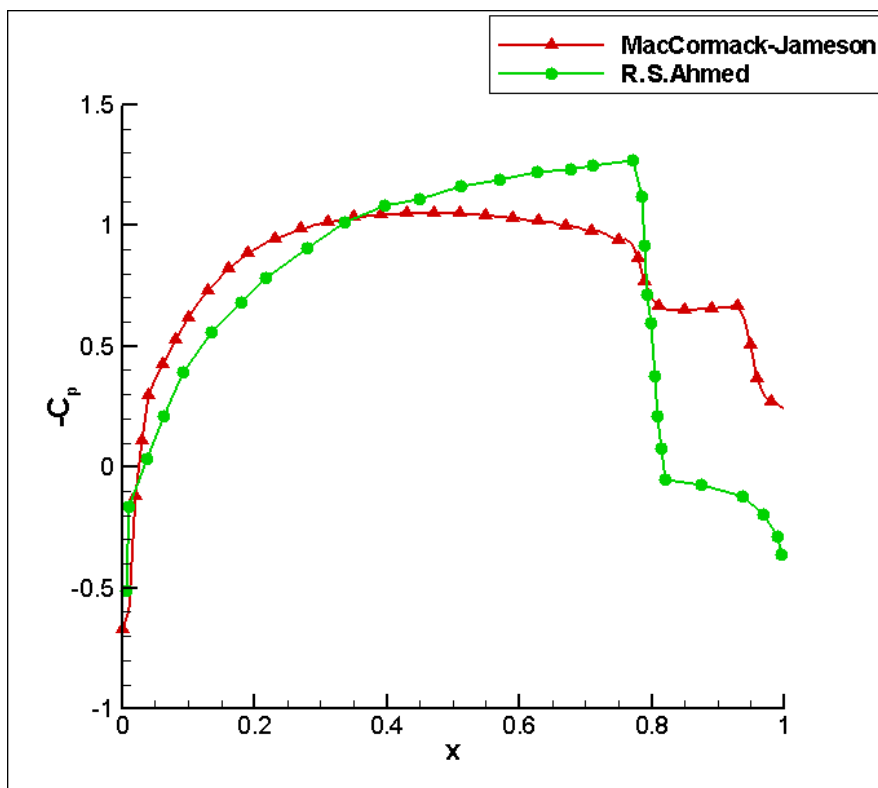

Figure 4.17 C_p distributions over NACA 0012 airfoil for inlet Mach number. 0.8(AOA 0^0)

From Fig. 4.17 it can be noticed that the coefficient of pressure over an airfoil is in close agreement with the results given in R.S.Ahmed [20]; although the shock is quite captured with the reasonable precision as to location, it's strength is underestimated by the present computations(possibly due to too much artificial viscosity).

4.3.3   Inlet Mach number 1 with angle of attack (AOA) 0^0:-

For this test case first type of mesh is used.

Initial conditions:-

Table 4.5 Initial conditions for Mach number. 0.5(AOA 0^0) flow over NACA 0012

$\rho^{'}$	0.6339
$p^{'}$	0.5283
$T^{'}$	0.8333
$u^{'}$	0.9128
$v^{'}$	0

Boundary conditions:-

Table 4.6 Boundary conditions for Mach number. 1(AOA 0^0) flow over NACA 0012

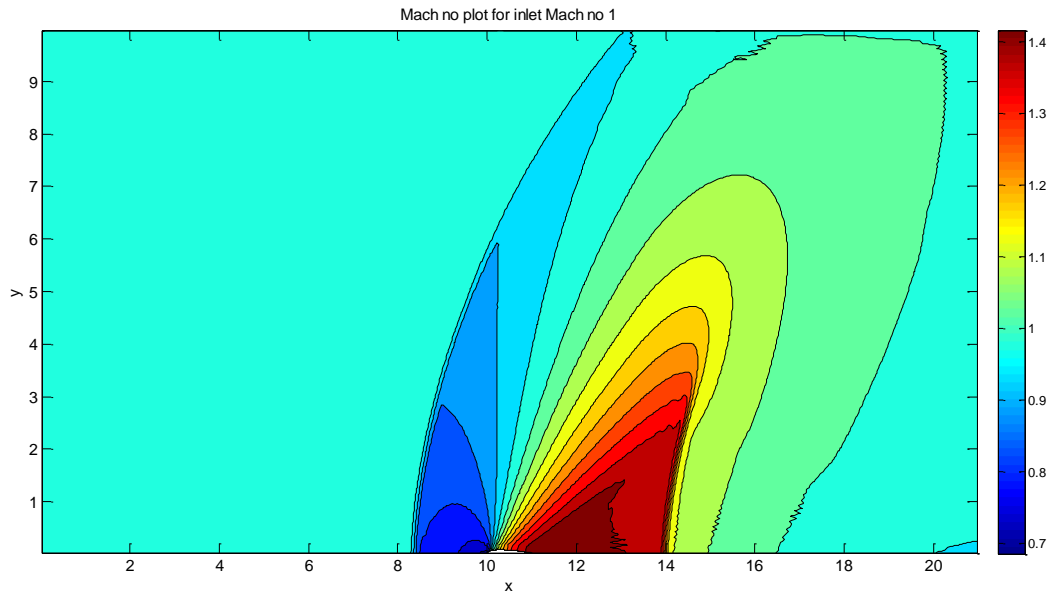|	Farfield boundary	Outlet
$\rho^{'}$	0.6339	All conservative variables are extrapolated from interior domain
$\rho^{'}u^{'}$	0.6339*0.9128	
$\rho^{'}v^{'}$	0	
$T^{'}$	0.8333	

Results of inlet Mach number 1 are as follows,

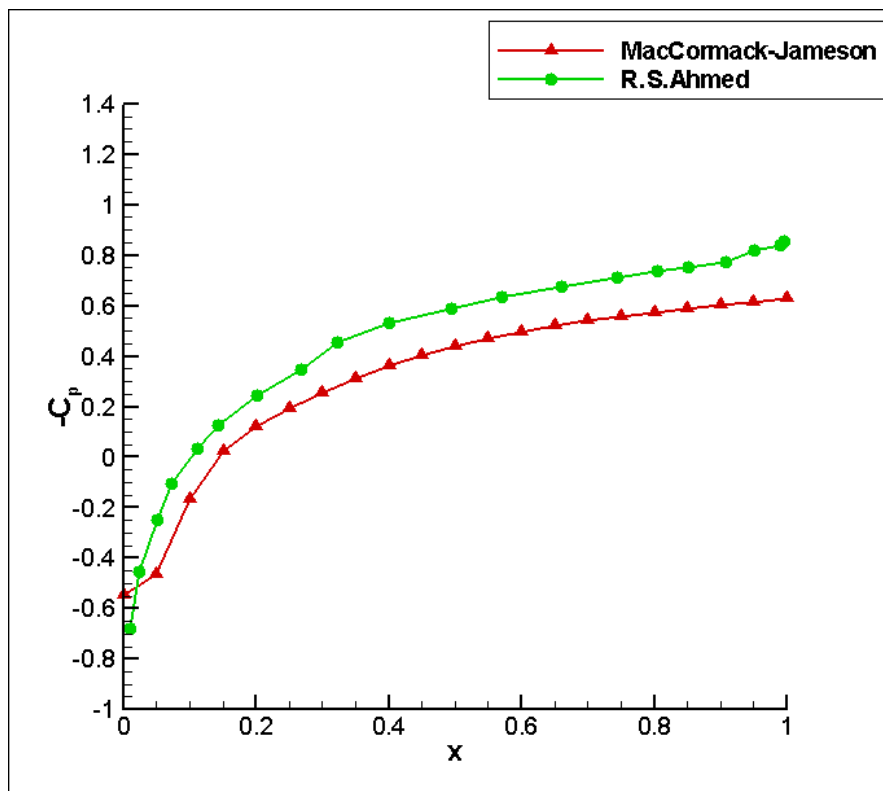Figure 4.18 Contour plot of Mach number 1 over NACA 0012 airfoil for inlet Mach number 1 (AOA 0^0).

Figure 4.19 C_p distributions over NACA 0012 airfoil for inlet Mach number 1(AOA 0^0)

From Fig. 4.19 it can be noted that the coefficient of pressure is in close agreement with the results given by R.S.Ahmed [20].

4.3.4   Inlet Mach number 1.2 with angle of attack (AOA) 0^0:-

For this test case first type of mesh is used.

Initial conditions:-

Table 4.7 Initial conditions for Mach number. 1.2(AOA 0^0) flow over NACA 0012

$\rho^{'}$	0.5311
$p^{'}$	0.4124
$T^{'}$	0.7764
$u^{'}$	1.057
$v^{'}$	0

Boundary conditions:-

Table 4.8 Boundary conditions for Mach number. 1.2 (AOA 0^0) flow over NACA 0012

	Farfield boundary	Outlet
$\rho^{'}$	0.5311	All conservative variables are extrapolated from interior domain
$\rho^{'}u^{'}$	0.5311*1.057	
$\rho^{'}v^{'}$	0	
$T^{'}$	0.7764	

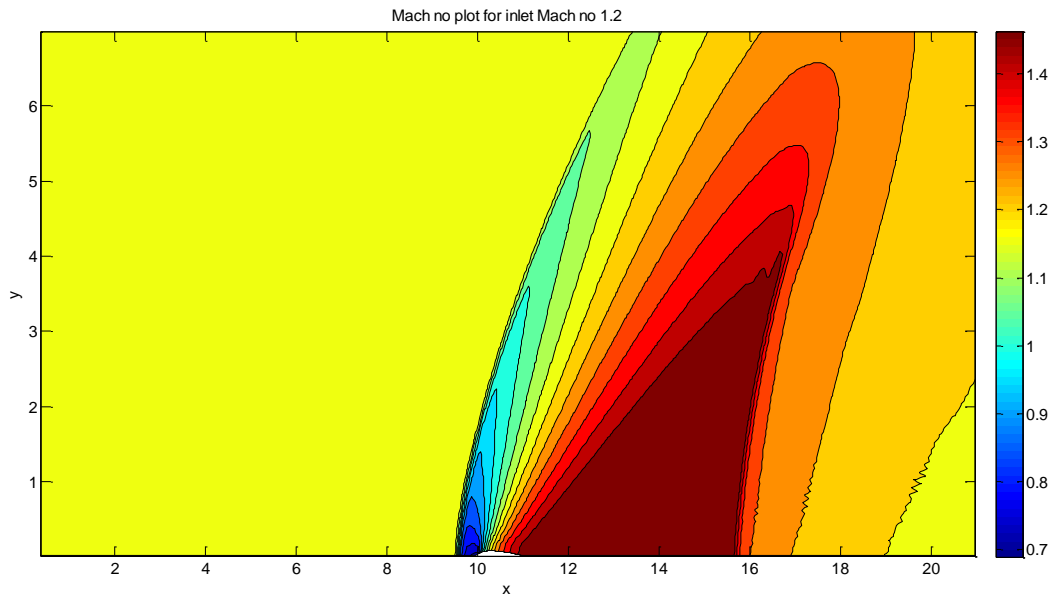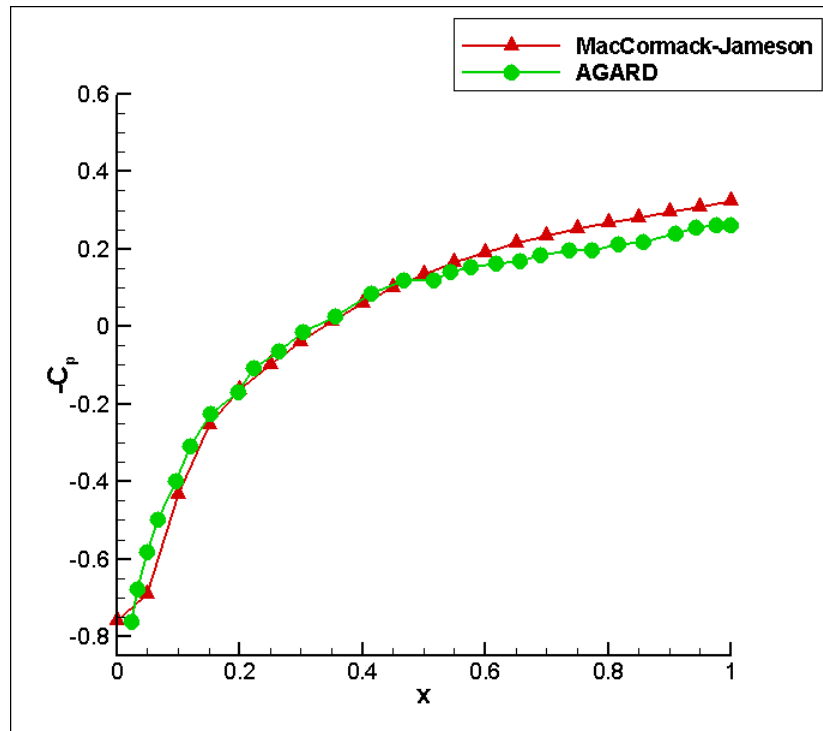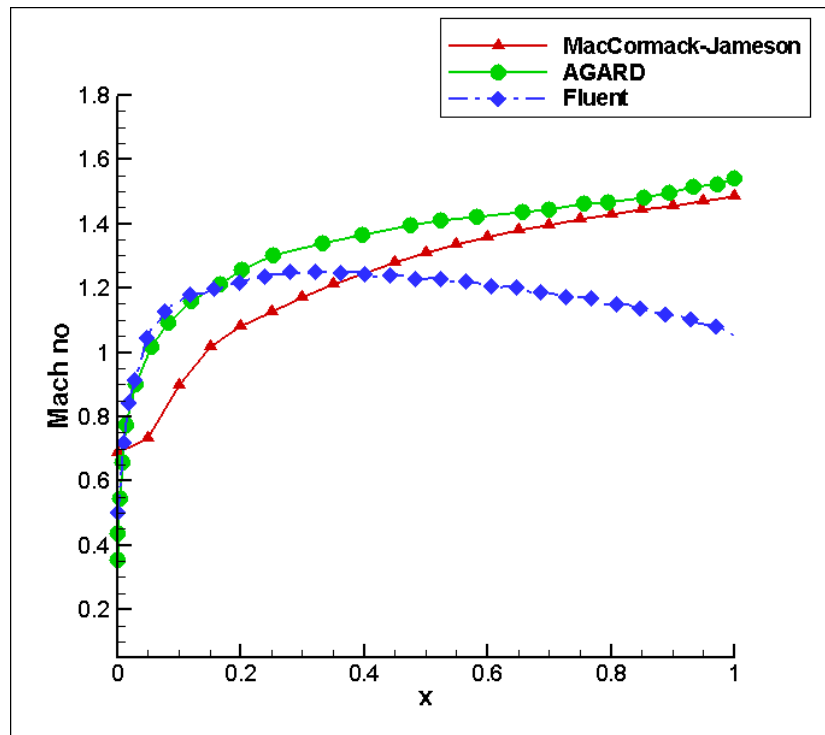Results of this case are as follows,

Mach no plot for inlet Mach no 1.2

Figure 4.20 Contour plot of Mach number1 over NACA 0012 airfoil for inlet Mach no. 1.2 (AOA 0^0).

(a)

(b)

Figure 4.21 C_p (a) and Mach number (b) distribution over NACA 0012 airfoil for inlet Mach number. 1.2 (AOA 0^0)

From Fig.4.21 it can be noted that coefficient of pressure is in good agreement with results given by AGARD (in FluSol software brochure) [21] and [20]. Mach number distribution is also in close agreement with results given by [21] while results from Fluent software show a quite different trend.

Closure:

Results obtained from the present study for pseudo 2-D nozzle problems are in good agreement with the results of Quasi 1-D results. The 2-D results of subsonic to supersonic flow shows quite significant differences with the Quasi 1-D results, while for the subsonic to subsonic flow case both results are in reasonable close agreement. Results of external flow over NACA 0012 airfoil for different Mach numbers are compared with the results given in the literature and they are in reasonably close agreement.

By TVD-MacCormack scheme 2-D subsonic to subsonic flow through a convergent nozzle has been solved. For the external flows over NACA 0012 airfoil, the TVD-MacCormack scheme was not attempted, due to lack of time. The variant MacCormack schemes discussed earlier become numerically unstable in the 2-D test cases.

Chapter 5

Conclusion and scope for future work

5.1   Conclusion

In the present study numerical computation of compressible fluid flow has been done. One dimensional problems i.e., shock tube, and Quasi 1D flow convergent divergent and convergent nozzles for subsonic to supersonic, subsonic to subsonic with and without shock have been solved. The results of these cases are compared with the results given in the literature and they are in good agreement. MacCormack scheme with Jameson's artificial viscosity has been implemented to solve 2D Euler equations. Quasi 1D nozzle problems are extended to 2D problems and these 2D problems for subsonic to supersonic and subsonic to subsonic flow without shocks have been solved. Results of these problems show similar, but not identical, behavior to that of Quasi 1-D nozzle flow problem results. Test cases of 2D external flow over NACA 0012 airfoil for inlet Mach no. of 0.5, 0.8, 1, and 1.2 have been solved using MacCormack scheme with Jameson's artificial viscosity and the results are validated with results given in literature, which are in reasonably close agreement. An attempt was also made to implement variants of MacCormack scheme in explicit and semi-implicit form, but it was found that they become numerically unstable in the 2-D test cases being solved.

5.2   Scope of future work

MacCormack scheme with Jameson's artificial viscosity have been implemented for 2D flows; this scheme can be further extended to 3D flows. The currently implemented schemes are for Euler equations, these equations suffer from numerical instabilities due to their lack of stabilizing viscous terms. Those schemes can be extended for Navier Stokes equations which may minimize the problem of numerical instability. High speed flows include turbulent effects, but the current implementation does not have a turbulence model; so a turbulence model can be implemented along with Navier stokes equations. In the present study the variants of MacCormack scheme that have been studied showed numerical instability which grows in time and blows up the solution. Further investigation is needed in

this regard. Study of adding artificial viscosity by a TVD scheme has been done but not implemented for 2-D external flow cases. So TVD-MacCormack scheme can be implemented for the Euler equations.

References

[1] *Computational Gas dynamics by* Culbert B. Laney

[2] *Modern Compressible flow* by John D. Anderson Jr.

[3] Numerical Computation of Internal and External flows by Charles Hirsch

[4] Computational Fluid Dynamics by T. J. Chung.

[5] Lax, P. D. Weak solutions of nonlinear hyperbolic equations and their numerical computation. Comm. Pure Appl. Math.,7, (1954)159–93.

[6] Lax, P. D. Hyperbolic systems of conservation laws and mathematical theory of shock waves. Society for Industrial and Applied Mathematics. Philadelphia, PA(1973).

[7] Lax, P. D. and Wendroff, B. Systems of conservation laws. Comm. Pure Appl. Math., 15, (1960). 363.

[8] MacCormack, R. W. The effect of viscosity in hypervelocity impact cratering. AIAA Paper, (1969). 66–354.

[9] MacCormack, R. W. and Paullay, A. J. Computational efficiency achieved by time splitting of finite difference operators. AIAA Paper. (1972) 72–154.

[10] MacCormack, R. W. A numerical method for solving the equations of compressible viscous flow, AIAA Paper, (1972) 81–0110.

[11] Courant, R., Isaacson, E., and Reeves, M.. On the solution of nonlinear hyperbolic differ-ential equations by finite differences. Comm. Pure Appl. Math., 5, (1952), 243–55.

[12] Steger, J. L. and Warming, R. F.. Flux vector splitting of the inviscid gas-dynamic equations with applications to finite difference methods. J. Comp. Phys., 40, (1981), 263–93.

[13] Van Leer, B. Towards the ultimate conservative difference scheme. I. The quest of monotonicity. Lecture Notes in Physics, Vol. 18, 163–68. Berlin: Springer Verlag. (1981)

[14] Pavel KRYŠTŮFEK, **Karel KOZEL Numerical simulation of compressible steady flows in 2D channel, Journal of applied science in the thermodynamics and fluid mechanics, Vol. 1, No. 1/2007, ISSN 1802-9388.

[15] Petra Puncochárová Porízková et. al, Simulation of unsteady compressible flow in a channel with vibrating walls -Influence of the frequency, Computers & Fluids 46 (2011) 404–410.

[16] J. Fürst, M. Janda, and K. Kozel: Finite volume solution of 2D and 3D Euler and Navier–Stokes equations. Math. Fluid Mechanics (J. Neustupa and P. Penel, eds.), Birkhäuser Verlag, Basel 2001. MR 1865053

[17] Jan Vimmr, Modelling of complex clearance flow in screw-type machines, Mathematics and Computers in Simulation 76 (2007) 229–236,2007.

[18] D. M. Causon. High resolution ⁻nite volume schemes and computational aerody-namics. In Josef Ballmann and Rolf Jeltsch, editors, Nonlinear Hyperbolic Equations Theory, Computation Methods and Applications, volume 24 of Notes on Numerical Fluid Mechanics, pages 63-74, Braunschweig, March 1989. Vieweg.

[19] Kreiss, H. O. Initial boundary value problem for hyperbolic systems. Comm. Pure Appl.Math., 23[1970]., 273–98.

[20] Whitfield, D.L.; Janus, J.M.: Three-Dimensional Unsteady Euler Equations Solution Using Flux Vector Splitting. AIAA Paper 84-1552, 1984.

[21] Rudy, D. H. and Strickwerda, J. C. [1980]. A non-reflecting outflow boundary condition for subsonic Navier-Stokes calculations. J. Comp. Phys., 36, 55–70.

[22] Gustafsson, B. [1982]. The choice of numerical boundary conditions for hyperbolic systems. J. Comp. Phys., 48, 270–83.

[23] Dutt, P. [1988]. Stable boundary conditions and difference schemes for Navier-Stokes equations.SIAM J. Num. Anal., 25, 245–67.

[24] Oliger, J. and Sundsr ¨om, A. [1978]. Theoretical and practical aspects of some initial boundary value problems in fluid dynamics. SIAM J. Appl. Math., 35, 419–46.

[25] Sod, G. A. 1978, Journal of Computational Physics, 27, 1-31

[26] R.S.Ahmed, Eng. & Tech. Journal, Vol. 29, No.5, 2011

[27] FluSol solver brochure.